ELSEVIER

Seminars in
ULTRASOUND
CT *and* MRI

Ultrasound in Dermatology: Why, How, and When?

Ximena Wortsman, MD

Nowadays, there are several applications of ultrasound in the field of dermatology, and the numbers continue to grow. This imaging technique can allow the study of the skin, the nail, and even the hair. The objective of this review is to provide an insight into the reasons for performing this examination, including technical considerations, the sonographic anatomy, and to discuss the sonographic characteristics of common dermatologic entities.
Semin Ultrasound CT MRI 34:177-195

The applications of ultrasound in dermatology have been growing in recent years due to the development of a newer generation of machines that work with high and variable-frequency probes that allow optimal definition of the superficial structures. These include common dermatologic entities that can easily benefit from the detailed anatomical data provided by sonography which may support diagnosis and management.

The skin is both the largest organ of the body and an exposed structure; therefore, any injury to it may easily affect the self-esteem and quality of life of individuals. The skin reveals several characteristics of a person such as age, gender, ethnicity, and health. It is also a complex organ that performs essential processes like healing, regulation of temperature, and storage of water, fat, and vitamin D. The appendages such as nails and hair are also crucially embedded in the integumentary system and play an active role. The nail unit is an enthesis that is closely connected with the distal insertion of the lateral bands of the extensor tendon and may be easily affected by any pathology that occurs in the distal interphalangeal joint. Moreover, the hair supports thermoregulation and plays a protective and social role for individuals.[1,2]

On the first hand, ultrasound in dermatology started with the usage of fixed-frequency equipments (20-100 MHz) that were capable of distinguishing the skin layers; hence, several studies on cutaneous pathologies have been performed using this technology.[3,4] Nevertheless, fixed-frequency machines present low penetration (5-6 mm at 20 MHz, 3 mm at 75 MHz, and 1 mm at 100 MHz) and lack color Doppler capabilities. This penetration issue may be relevant because normal skin presents variable thicknesses according to the corporal segment. For example, only the dermis in the dorsal region can measure >3 mm (thickness) which anatomically may impede the detection of deeper lesions with fixed-frequency probes. Furthermore, the latter characteristics may be critical, for example in the diagnosis of skin cancer or vascular anomalies.[2,5,6] These fixed-frequency ultrasound machines are available in some Departments of Dermatology and research units and can provide valuable information if the limitations are kept in mind.

On the other hand, the variable-frequency equipments that are used for studying the skin are usually incorporated in sophisticated and expensive multichanneled ultrasound machines with powerful processors and probes that have an upper frequency range that currently varies from 15-22 MHz. These equipments show sensitive color and power Doppler, as well as light probes that can successfully adapt to the skin contours in the different parts of the body. Moreover, hockey stick-shaped probes allow an adequate attachment to the surface when exploring complex corporal segments, such as the face, the tongue, the ear pinna, or the fingernails.

The advantages of variable-frequency ultrasound are the reasonable balance between penetration and resolution, the real-time capability, as well as the possibility of identifying and measuring both texture and blood flow changes. The limitations of this technique are the measurement of ≤0.1 mm lesions, the detection of pigments such as melanin, and the detection of flat epidermal-only lesions.[5]

The information provided on sonographic examination should ideally be different or complementary to that already deduced by a well-trained physician clinically. Thus, reports of the dermatologic applications of sonography include relevant anatomical data on the extension, exact location, vascularity, activity, and severity of common cutaneous abnormalities. This information can potentially allow modifying management (medical or surgical planning), prevent recurrences, and discriminate between a dermatologic or

Department of Radiology and Department of Dermatology, Clinica Servet, Faculty of Medicine, University of Chile, Santiago, Chile.
Address reprint requests to Ximena Wortsman, MD, Department of Radiology and Department of Dermatology, Clinica Servet, Faculty of Medicine, University of Chile, Almirante Pastene 150, Providencia, Santiago, Chile. E-mail: xwo@tie.cl

0887-2171/$-see front matter
http://dx.doi.org/10.1053/j.sult.2012.10.001

nondermatologic origin. Moreover, subclinical changes can be traced without the need to inject a contrast medium (at least in baseline studies) and in a safe environment that lacks radiation issues or confinement in reduced spaces.[2,5,6]

These considerations should be added to the fact that nowadays, highly informed patients demand the best cosmetic results besides the correct management of their diseases.

The aim of this review is to provide an insight into why this type of examination may be needed, supply a basic guideline about how to perform it, considering the technical requirements and the normal anatomy, and lastly, analyze when this imaging modality would be applied in common dermatologic entities, highlighting their sonographic characteristics.

Technical Considerations

For dermatologic applications, we use high-resolution equipments that work with variable-frequency probes. Ideally, the recommended frequency for studying this field is $\geq$15 MHz. Nevertheless, this comment does not denigrate the usage of lower frequencies but emphasizes the fact that the definition of the skin layers improves at higher frequencies.

In our department, sedation (chloral hydrate 50 mg/kg) is used approximately 30 minutes before the ultrasound examination in children $<$4 years, after informed consent is signed by the parent or guardian. This medication prevents the artifacts that are derived from crying or movements and provides a quiet, comfortable, and safe environment for the test. A modified Aldrete scoring (ie, evaluation of activity, respiration, circulation [blood pressure], consciousness, and oxygen saturation) is used for monitoring the children in the Department and they are discharged with $\geq$9 points.[7]

We use the technique, that has already been reported, for studying localized lesions of the skin that consists first, in the inspection of the lesion, and then the application of a copious amount of gel over the lesional area. Gray scale followed by color or power Doppler ultrasound or both is performed in at least 2 perpendicular axes. Detection of the echogenicity patterns, measurement of the size, identification and measurement of the blood flow (distribution, type, and maximum peak systolic velocity of the arterial vessels), localization and the identification of deeper layer involvement are reported. In the presence of asymmetric lesions, the deepest part is considered to measure the thickness during the sonographic examination.[2,5,6]

In the nail unit, the examination includes both the ungual and periungual regions.[9] In the scalp, displacement of the hair tracts is performed for optimizing contact between the skin and the probe.[2,6,8,9]

The examination requires a variable degree of illumination in the room, thus strong lighting is used for inspecting the lesion, and a dimmer that allows the room to be darkened during the test is usually used. In the presence of multiple lesions, sequential lighting and darkening of the room is performed to properly locate the probe in the lesional area.

The settings of the machines include power Doppler to detect slow flow, the lowest repetition pulse frequencies and wall filters, as well as color gain below the noise threshold that does not cause artifacts.

Three-dimensional reconstructions (5-8 second sweeps) and color filtering are commonly used to improve the presentation and highlighting the findings.[2,5,6]

Sonographic Anatomy

The skin is composed of 3 layers: epidermis, dermis, and hypodermis, which is also called subcutaneous tissue. Even though the epidermis has an ectodermal origin, and the dermis and hypodermis have a mesodermal origin, these layers are deeply functionally connected. Hence, the involvement of one layer may secondarily affect the other, and many of the pathologies in dermatology involve more than one layer.

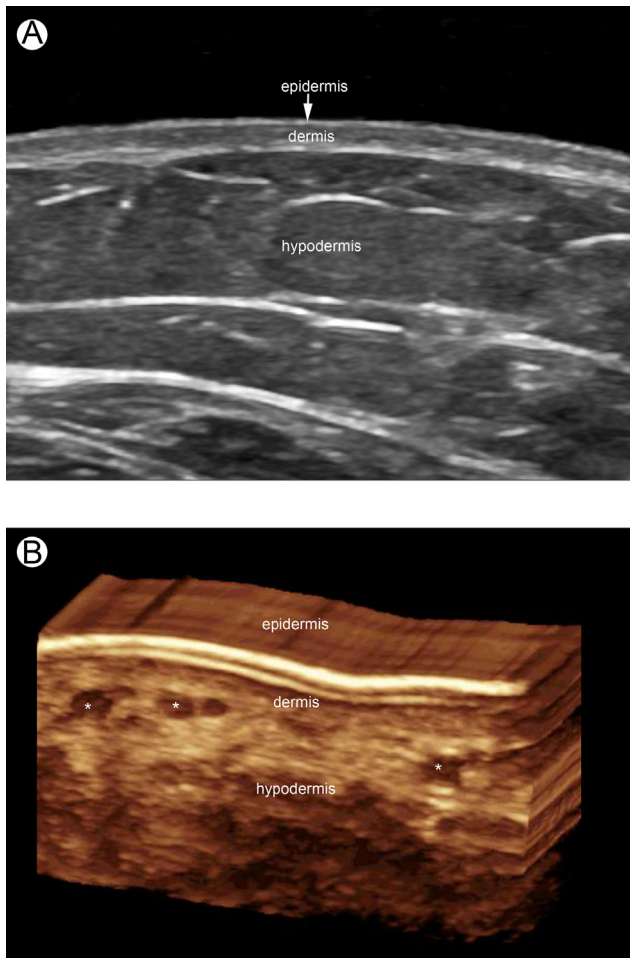

Figure 1 Sonographic anatomy of the skin. (A) Nonglabrous skin (gray scale ultrasound, transverse view, ventral forearm) shows the morphology of the skin layers. (B) Glabrous skin (3D reconstruction, transverse view, and plantar region) demonstrates the thick and bilaminar hyperechoic appearance of the plantar epidermis. *, venous vessels. (Color version of figure is available online.)

The echogenicity of the skin layers is influenced by their components. Thus, keratin affects the echogenicity of the epidermis, collagen affects the echogenicity of the dermis, and the fatty lobules provide the main echogenicity of the hypodermis. The epidermis shows in nonglabrous skin (ie away from the palms of the hands and soles of the feet) as a hyperechoic line. In contrast, in glabrous skin (i.e. the palms and soles), the epidermis presents as a bilaminar parallel hyperechoic structure. The dermis shows as a hyperechoic band, less bright than the epidermis. The hypodermis presents as hypoechoic fatty lobules separated by hyperechoic fibrous septa.[2,5,6] (Fig. 1).

During the aging process, a hypoechoic band in the upper dermis called subepidermal low-echogenicity band (SLEB) can be detected in the corporal regions exposed to the sun, such as the face and the dorsal forearm. Thus, the SLEB has been proposed as a marker for estimating the effects of photoaging.[10]

With the current technology, low-flow arterial and venous vessels are detected in the hypodermis, and occasionally in the dermis.

The nail region is composed of the nail unit and the periungual zone. The nail unit comprises 3 parts: the nail bed, the plates (dorsal and ventral), and the matrix. The nail bed is a hypoechoic area that may become slightly hyperechoic in the proximal third beneath the ungual matrix. The nail plate is composed of keratin and shows as a bilaminar hyperechoic structure with a dorsal and a ventral aspect, also called dorsal and ventral plate. In between the plates there is a virtual hypoechoic space, called the interplate space. The origin of the nail plates is located distally to the level of the distal interphalangeal joint. The periungual region comprises the skin of the proximal and lateral nail folds, as well as the hyponychium (distal part) that shows an echostructure similar to the one previously described for the cutaneous layers, but without fatty lobules. The bony margin of the distal phalanx shows as a hyperechoic line beneath the nail bed. Neighboring the nail is the insertion of the lateral bands of the extensor tendon that are located at the base of the distal

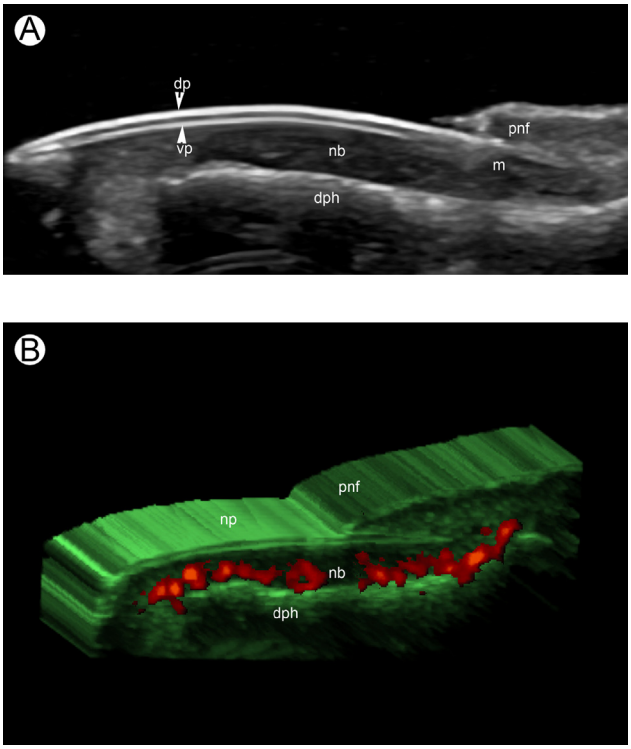

Figure 2 Sonographic anatomy of the nail. (A) Gray scale ultrasound (longitudinal view) demonstrates the parts of the nail unit. (B) 3D power angio reconstruction (longitudinal view) shows the blood flow in the nail bed. nb, nail bed; dp, dorsal plate; vp, ventral plate; np, nail plates; pnf, proximal nail fold; dph, distal phalanx; m, matrix region. (Color version of figure is available online.)

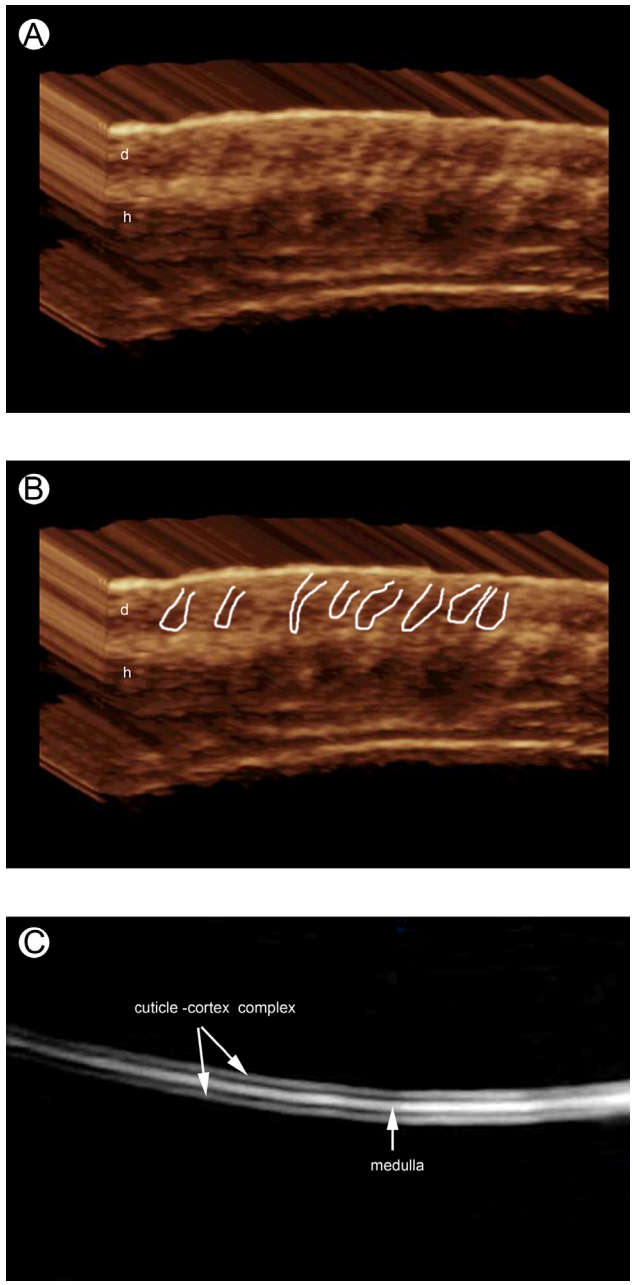

Figure 3 Sonographic anatomy of the scalp and scalp hair. (A, B) 3D reconstructions of the scalp skin; in (B), the hair follicles were outlined. (C) Anatomy of the scalp hair (gray scale, longitudinal view). (Color version of figure is available online.)

phalanx. This appears as a hyperechoic band with a fibrillar pattern. The distal interphalangeal joint shows up as a hypoechoic space between the hyperechoic bony margins of the distal and the middle phalanx. Low-velocity arterial and venous vessels are detected in the nail bed, usually close to the bony margin[2,6,8,11,12] (Fig. 2).

The hair comprises 2 parts: the hair follicle (the nonvisible part) and the hair tract (visible part). The hair follicles in the scalp present as hypoechoic oblique bands that show a variable degree of depth, according to the phase of the follicle. Thus, although the immature hair follicles (telogen phase) are located in the upper dermis (subepidermal region), the mature hair follicles (anagen phase) are found in the lower dermis adjacent to the upper hypodermis. Hence, the hair follicles pass through a growth cycle, also called the "hair cycle clock" that goes from telogen (resting phase) to anagen (active mature phase) with an in-between stage called catagen.[9,13] The orientation of the hair follicles can change according to ethnic parameters. Thus, they tend to show a more pronounced obliquity in Caucasians, can be almost parallel in individuals with African ancestry, and present a more vertical orientation in persons with Asian ancestry.[14]

The hair tract is mainly composed of layers of keratin. In the scalp, the hair tract mostly presents as a trilaminar hyperechoic structure with 2 outer layers, the cuticle-cortex complex, and an inner layer called the medulla. In contrast, the tracts of the villous hair which includes the eyelashes and eyebrows show as hyperechoic linear bands. The difference in appearance between the scalp and the villous hair tracts may be due to structural variations or the level of definition of the currently available technologies or both.[9]

The scalp shows a centripetal blood flow network that mainly comes from branches of the external and internal carotid arteries, predominantly from the temporal and occipital arteries. These branches sequentially decrease in size, going from the lateral to the medial region. Commonly, low-flow arteries and veins are detected in the hypodermis and running through the galea (the aponeurosis and muscle layer) close to the bony margin of the skull[15] (Fig.3).

Skin Pathology

Benign Lesions

Cysts

Epidermal Cyst. These cystic lesions are derived from the entrapment of epidermal components in the dermis and hypodermis. Epidermal cysts may be due to embryologic, traumatic, or postsurgical causes. Histologically, epidermal cysts are composed of stratified epithelium with a granular layer, and they contain keratin. They do not show sebaceous components and therefore, the name "sebaceous cyst" is confusing and does not represent the real nature of these structures.

On sonography, the appearance of epidermal cysts can vary according to the phase of the cyst. Thus, intact epidermal cysts show as well-defined, oval or round shaped, anechoic or hypoechoic structures in the dermis and hypodermis, that commonly present a connecting tract to the subepidermal region called "punctum". Rarely, hyperechoic lines due to fragments of hair tracts or hyperechoic spots due to calcium deposits are detected within the cyst. Occasionally, giant cysts that contain compact keratin can appear as hypoechoic, round- or oval-shaped structures that may present "onion-like" layers or "pseudotestes appearance" (ie, brighter inner echoes and anechoic filiform areas). Inflamed cysts are hypoechoic and larger in size, and ruptured cysts usually present an irregular or lobulated shape. Inflamed and ruptured cysts are commonly accompanied by increased

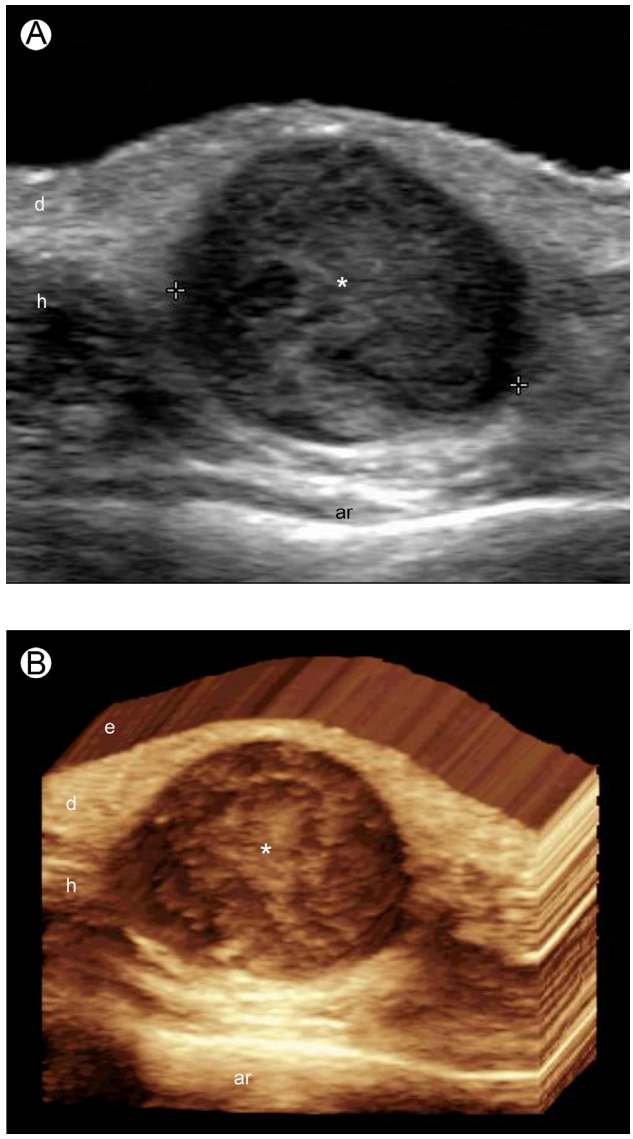

Figure 4 Intact epidermal cyst. (A) Gray scale ultrasound (longitudinal view, left cheek) demonstrates a well-defined, round-shaped hypoechoic structure (*, between marker) located in the dermis and hypodermis. Notice the posterior acoustic reinforcement artifact (ar). (B) 3D reconstruction (5-8 seconds sweep) highlighting the epidermal cyst (*). e, epidermis; d, dermis; h, hypodermis; ar, posterior acoustic reinforcement. (Color version of figure is available online.)

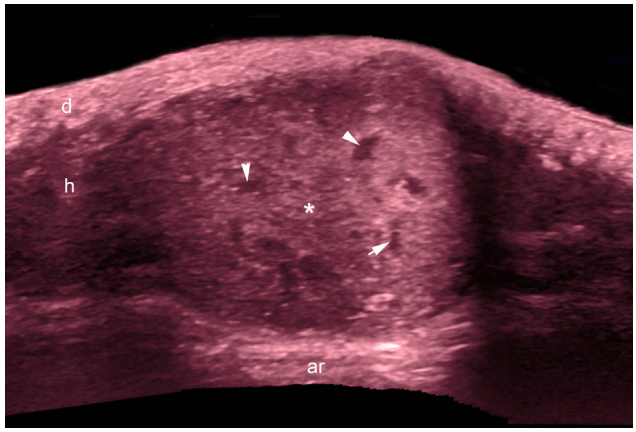

Figure 5 Epidermal cyst with "pseudotestes" pattern. Gray scale with color filter (longitudinal view, lumbar region) demonstrates a well-defined, oval-shaped, hypoechoic structure (*) located in the dermis and hypodermis. Notice the filiform anechoic areas (arrow and arrowheads) within the cyst and the posterior acoustic reinforcement artifact (ar). d, dermis; h, hypodermis. (Color version of figure is available online.)

echogenicity of the surrounding hypodermis, a sign of edema. The latter feature is more common in ruptured cysts because the keratin that is spread into the surrounding tissue produces a foreign body-like reaction. Irrespective of the phase of the cyst, frequently the posterior acoustic enhancement artifact, typical of fluid-filled structures, is conserved. On color or power Doppler, increased blood flow is detected, mainly in the periphery of inflamed or ruptured epidermal cysts. Usually the vascularity is composed of low-flow arterial or venous vessels[2,6,16–18] (Figs. 4–7).

Trichilemmal Cyst (TC). These are derived from the external sheath of the hair follicle and 90% of them are located on the scalp. Clinically TCs may present as bumps or lumps associated with focal alopecia. They are lined with cuboidal epidermal cells without a granular layer. TCs contain keratin, oily material, and sometimes hair fragments. On sonography, they show as single or multiple well-defined, anechoic or hypoechoic structures located in the dermis and hypodermis. Echoes within the cyst due to debris are usually detected. Usually, they do not show a connecting tract (punctum) to the subepidermal region. Occasionally, they may show a target appearance with a hypoechoic rim and hyperechoic center. This hyperechoic center is usually composed of highly compact hair tracts or calcium deposits or both. In the presence of inflammation, increased blood flow with low-flow vessels may be detected in the periphery of the cysts[9,19,20] (Fig. 8).

Pilonidal Cyst (PC). These cysts are usually seen in males and commonly in the intergluteal region. They can be related to trauma and the condition has been named "Jeep Disease". PCs seem to be the consequence of the penetration of hair tracts through the skin or dilated follicular ostia or both. Histologically, they are composed of a sinus lined with stratified squamous epithelium that contains a nest of hair fragments, granulation, and inflamed tissue. Frequently PCs tend to become infected and become abscesses that drain purulent material. On sonography they show as oval-shaped hypoechoic pseudocystic structures located in the dermis and hypodermis that present hyperechoic lines that correspond to hair-tract fragments. Commonly, they are connected with the base of the regional hair follicles, these being enlarged. Inflamed PCs show increased vascularity in the periphery. Importantly, ultrasound allows the detection of the extent, axis (oblique, longitudinal, or transverse), and branches of the cyst which may support surgical planning[2,6,21,22] (Fig. 9).

Solid Lesions

Pilomatrixoma. These benign tumors are derived from the hair matrix and are also called pilomatricomas, or calcifying epitheliomas of Malherbe. They are more common in children and young adults and are present in the head, neck, and extremities. On histologic examination, pilomatrixomas are composed of lobules

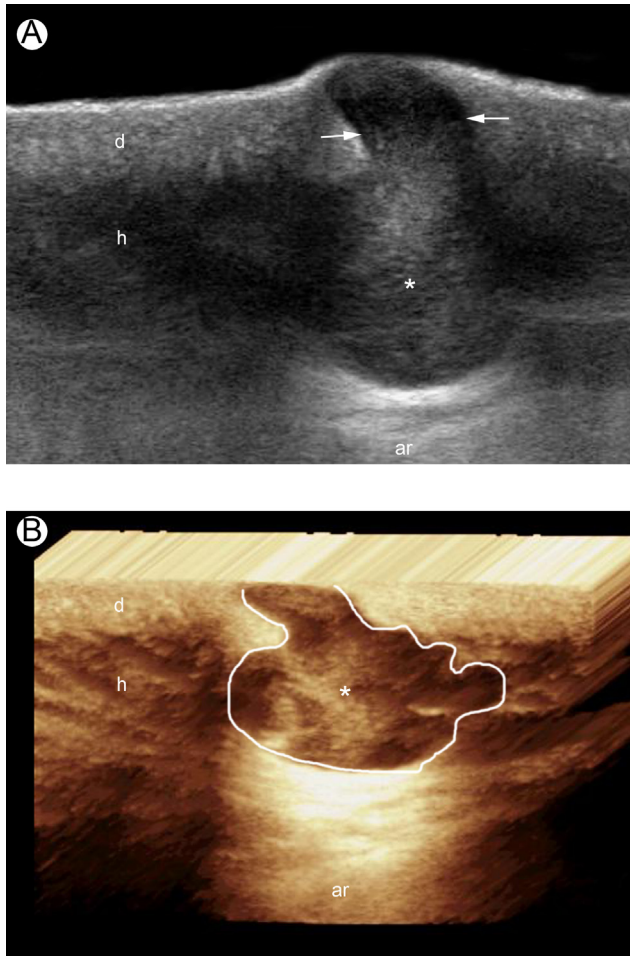

Figure 6 Epidermal cyst with punctum. (A) Gray scale ultrasound (transverse view, dorsal region) shows a well-defined, oval-shaped hypoechoic structure (*) located in the dermis and hypodermis. A connecting hypoechoic tract to the subepidermal region, called punctum (arrows), is observed in the upper part of the structure. (B) 3D reconstruction of the cyst (5-8 seconds sweep). d, dermis; h, hypodermis; ar, posterior acoustic reinforcement artifact. (Color version of figure is available online.)

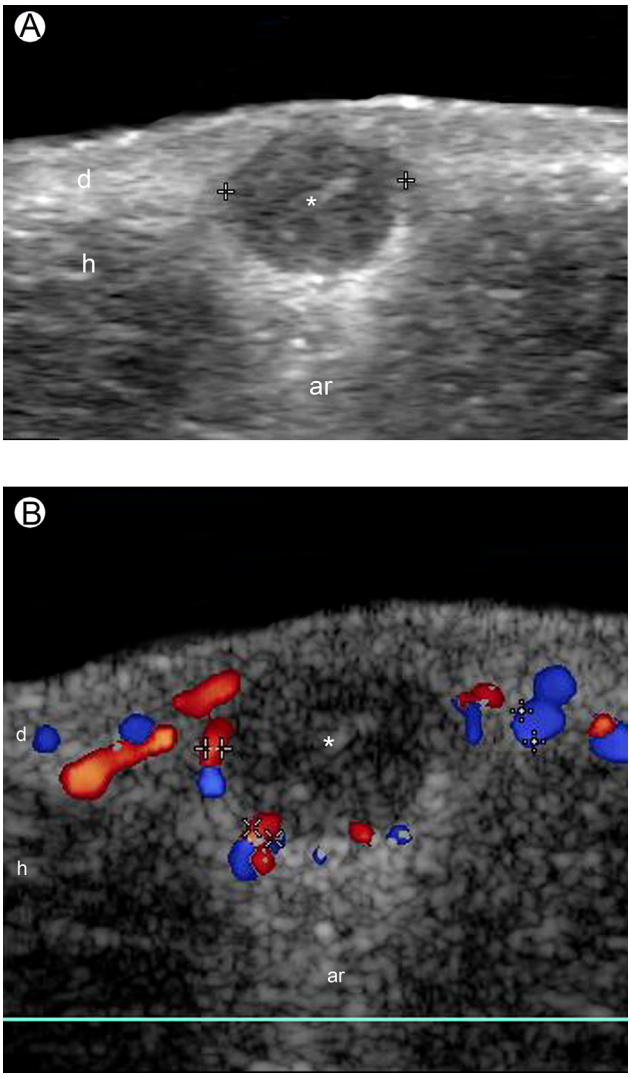

Figure 7 Epidermal cyst with inflammation. (A) Gray scale ultrasound (longitudinal view, right cheek) shows a round-shaped hypoechoic structure (*, between markers) that presents slightly irregular borders. (B) Color Doppler ultrasound (longitudinal view and right cheek) demonstrates increased vascularity in the periphery of the cyst. d, dermis; h, hypodermis; ar, posterior acoustic reinforcement artifact. (Color version of figure is available online.)

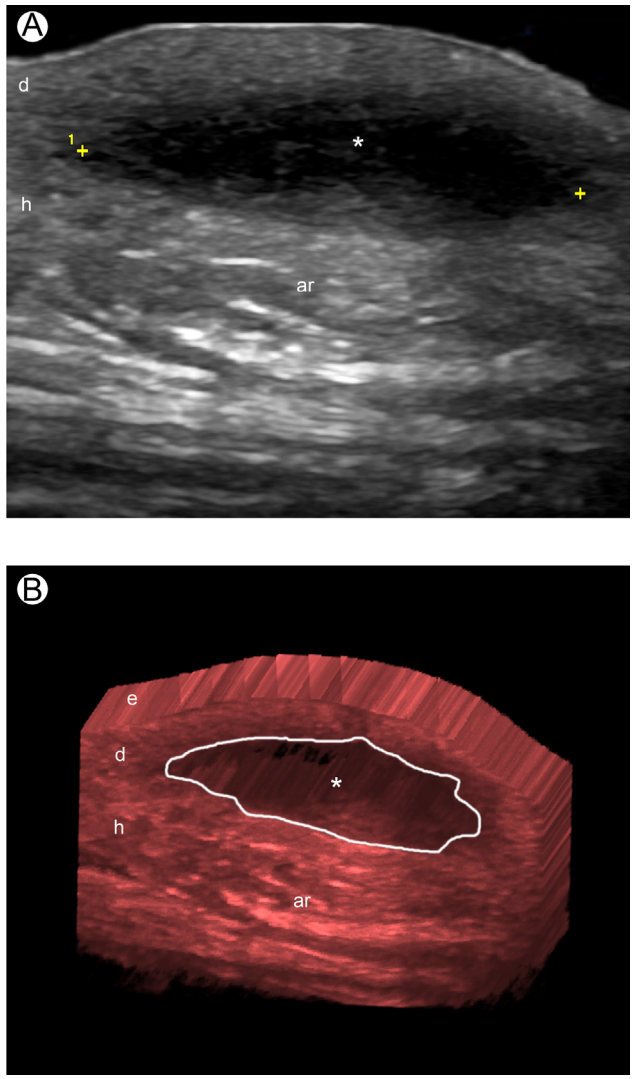

Figure 8 Trichilemmal cyst. (A) Gray scale ultrasound (longitudinal view) and (B) 3D reconstruction (5-8 seconds sweep, longitudinal view) demonstrates a well-defined, oval-shaped, anechoic structure (*, between markers) located in the dermis and hypodermis of the scalp (occipital region). Notice the posterior acoustic reinforcement artifact and the echoes (debris) within the cyst. e, epidermis; d, dermis; h, hypodermis. (Color version of figure is available online.)

with basaloid and ghost cells, calcifications, and eosinophilic keratinous debris that are surrounded by a fibrous pseudocapsule. Clinically, misdiagnosis has been reported in up to 56% of the cases.[2,6,23]

On sonography, they can show a wide range of appearances. The most common form of presentation is the "target nodule" (ie, hypoechoic rim and hyperechoic center) located in the dermis and hypodermis that shows hyperechoic spots in the center due to calcium deposits. Thus, these hyperechoic calcified spots usually present a posterior acoustic shadowing artifact. Calcium is a key element for diagnosing these tumors and has been reported in up to 80% of the cases.[24–28]

On color Doppler, pilomatrixomas show a variable degree of vascularity, ranging from hypovascular to hypervascular. The latter hypervascular form of presentation with strong outer (ie, at the rim) and inner (ie, at the center) blood flow may even simulate hemangiomas on physical examination. Other less common variants include the fully calcified pilomatrixoma, that shows as a hyperechoic nodule with strong posterior acoustic shadowing, and the cystic pilomatrixoma that presents as a anechoic cyst with an eccentric hypoechoic solid nodule that also shows tiny hyperechoic calcified spots surrounded by septa that connect the nodule with a hypoechoic thick, fibrous wall[2,6,23–28] (Figs. 10 and 11).

Dermatofibroma. This is a fibrous tumor that usually presents in the lower extremities or trunk in middle-aged females. It is also called fibrous histiocytoma and histiocytoma cutis. It is not clear if the origin of the lesion is a reaction to

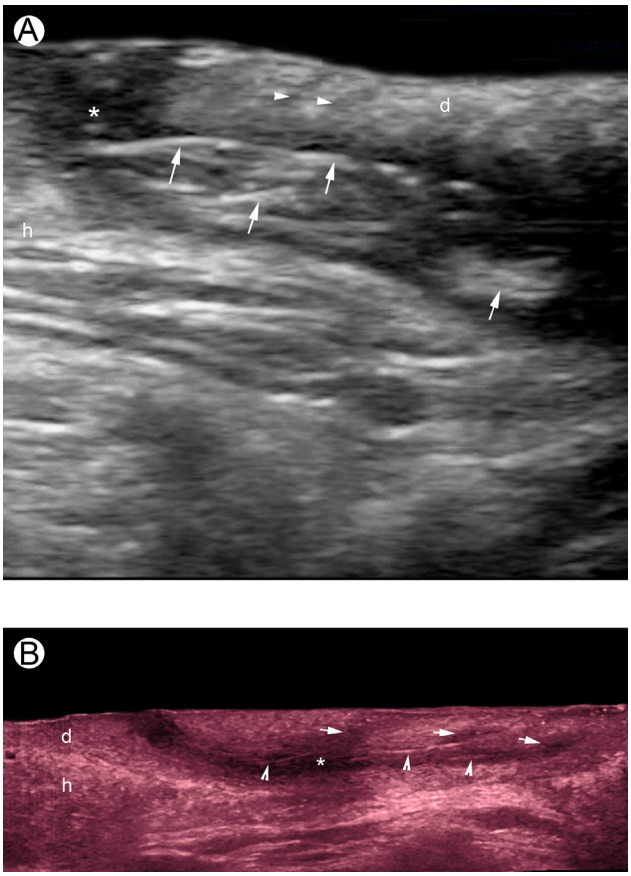

Figure 9 Pilonidal cyst. (A) Gray scale ultrasound (longitudinal view, intergluteal region) shows hypoechoic structure (*) located in the dermis and hypodermis. Notice the hyperechoic lines (arrows) that correspond to hair tracts fragments and the enlargement of the hair follicles (arrowheads) located on top of the cyst.(B) Gray scale ultrasound (extended field of view with color filtering) demonstrates an hypoechoic structure (*) running through the dermis and hypodermis. There are hyperechoic lines (arrowheads) that represent hair tracts fragments within the cyst. Notice the connection of the cyst to the base of 3 enlarged hair follicles (arrows) located on top of this structure. d, dermis; h, hypodermis. (Color version of figure is available online.)

trauma or insect bites or both, or directly neoplastic. Histologically, dermatofibromas are composed of spindle cells, hyaline collagenous stroma, scattered lipid-laden histiocytes, multinucleated giant cells, and hemosiderin deposits. On sonography, they show as ill-defined or oval-shaped hypoechoic or heterogeneous lesions or both that involve the dermis and less frequently the upper hypodermis. Commonly, a distortion and enlargement of the regional hair follicles is detected. The degree of vascularity is variable and can go from hypovascular to prominent blood flow with low-velocity vessels[6,29] (Fig. 12).

Vascular Anomalies

These are common causes of referral for sonographic examination. Vascular anomalies are usually cataloged by Mulliken and Glowacki's classification, proposed in 1982, that divides these conditions into 2 main entities: hemangiomas and vascular malformations, based on the clinical findings, evolution, histologic characteristics, and prognosis.[30,31]

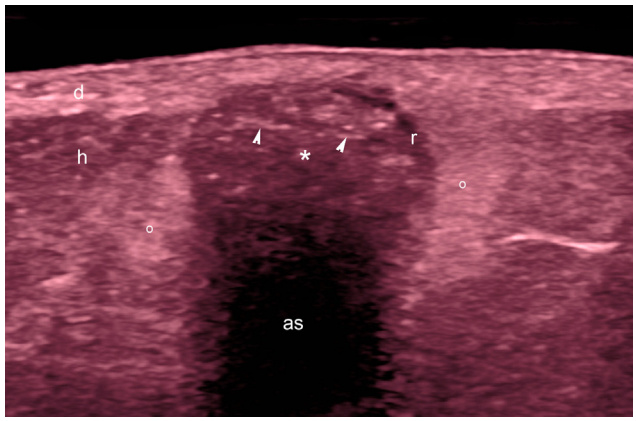

Figure 10 Pilomatrixoma. Gray scale ultrasound (transverse view with color filtering, left thigh) demonstrates "target nodule" (*) with an hypoechoic rim (r) and hyperechoic center that contains hyperechoic spots (arrowheads). Increased echogenicity of the surrounding hypodermis (o) is also detected. Additionally, a posterior acoustic shadowing artifact (as) could be recognized. d, dermis; h, hypodermis. (Color version of figure is available online.)

Hemangiomas of Infancy. These are the most common soft-tissue tumors in children and are composed of true endothelial proliferations. Clinically, they present a fast growth after birth and for the first 1 or 2 years and then a slow regression period that usually lasts for 4 or 5 years. These lesions commonly respond to medical treatments (systemic or topical). The sonographic appearance of hemangiomas differs according to the phase. Thus, during the fast growth phase they present as ill-defined hypoechoic solid tumors with strong vascularity. There are arterial and venous vessels and sometimes arteriovenous shunts. The arterial blood flow can be so prominent that occasionally it may reach very high peak systolic velocities that can present a similar velocity to the flow detected in a large size artery, such as the external carotid artery. During the partial regression phase, part of the hemangioma turns to hyperechoic and there is a decrease of the vascularity. In the total regression phase, the lesion becomes fully hyperechoic and hypovascular. Commonly at the end-stage phase, lipodystrophies (ie, abnormalities in the amount of the fatty tissue in the hypodermis which may be increased or decreased) can be detected in the lesional area[2,6,32,33] (Fig. 13).

Vascular Malformations. These are abnormal proliferations of vascular channels and do not compose a true tumor. They can be classified according to the type of vessels, into arterial, venous, capillary, lymphatic, or mixed. Also, they can be separated into high-flow (arterial and arteriovenous) and low-flow (venous, capillary, and lymphatic). On sonography, vascular malformations commonly present as a nest of anechoic ducts or lacunar cystic areas. Nevertheless, low-flow capillary malformations may present as hyperechoic islets in the hypodermis or hypoechoic areas in the dermis or

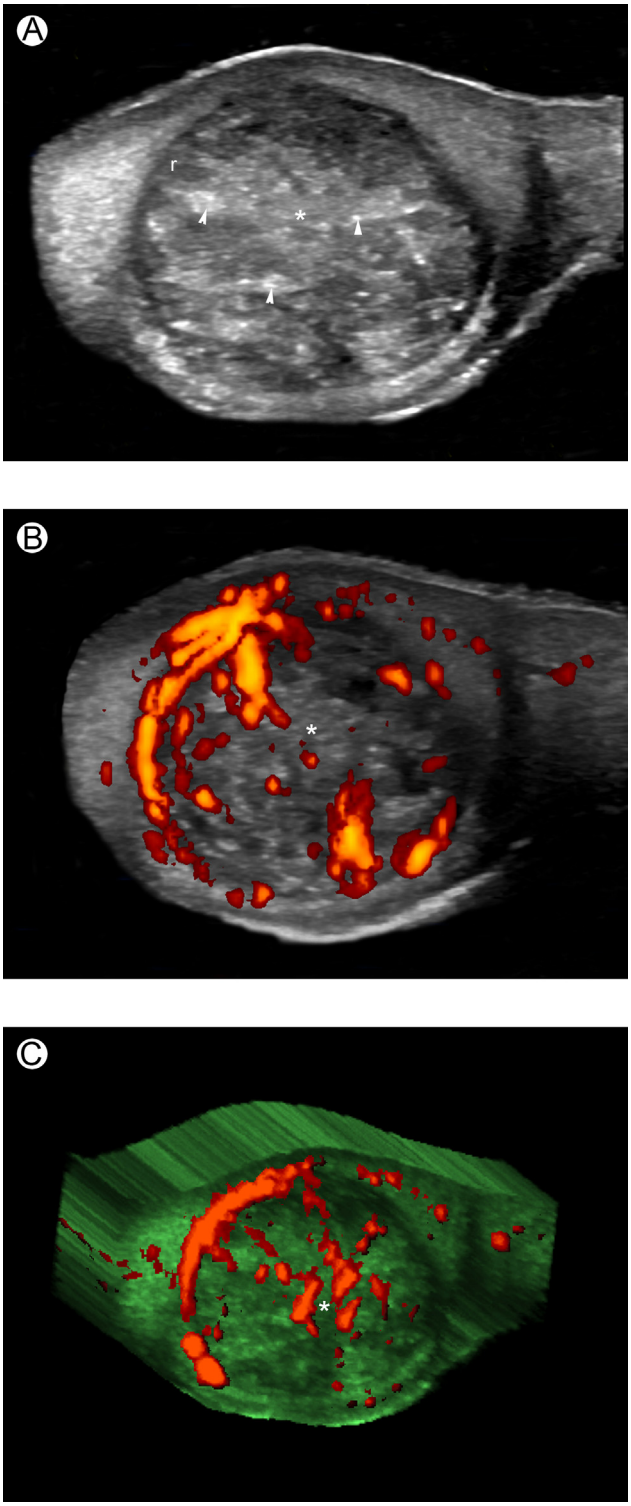

Figure 11 Pilomatrixoma. (A) Gray scale ultrasound (transverse view and the lobule of the right ear pinna) demonstrates a well-defined, round-shaped "target appearance" (ie, hypoechoic rim and hyperechoic center) lesion (*). Notice the hyperechoic spots (arrowheads) in the center of the lesion due to calcium deposits. (B) Power Doppler (transverse view) shows increased vascularity in the periphery and center of the lesion (*). (C) 3D power Doppler reconstruction of the lesion (*, transverse view, 5-8 seconds sweep) highlights the findings. r, rim. (Color version of figure is available online.)

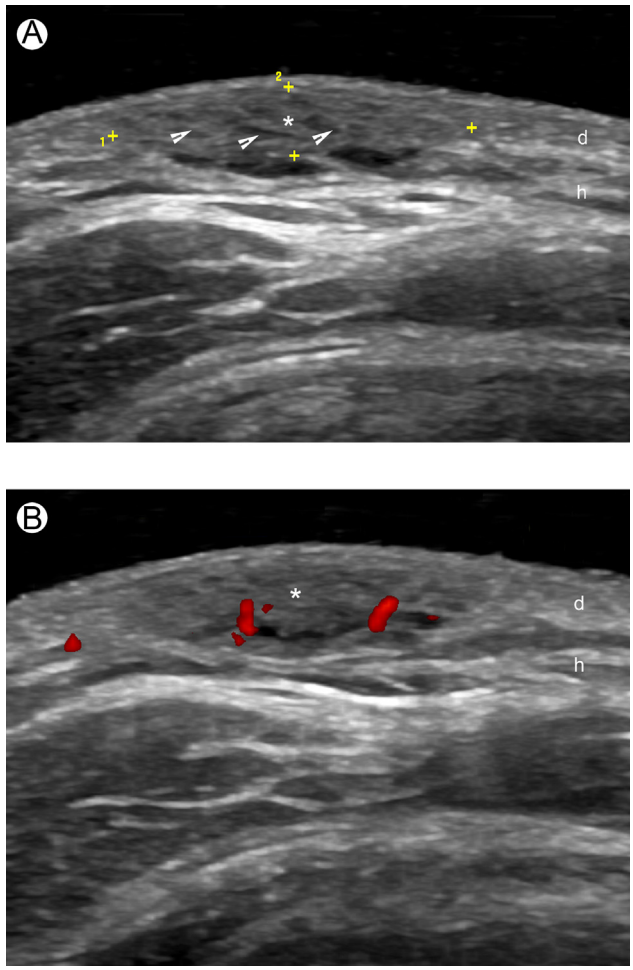

Figure 12 Dermatofibroma. (A) Gray scale ultrasound (transverse view, left shoulder) demonstrates ill-defined, oval-shaped hypoechoic and heterogeneous lesion (*, between markers) in the dermis and hypodermis. There is distortion of the regional hair follicles (arrowheads). (B) Power Doppler (transverse view) shows slightly increased vascularity within the lesion (*). d, dermis; h, hypodermis. (Color version of figure is available online.)

both. Flat, epidermal capillary malformations may increase the thickness of the epidermis or may show no sonographic abnormality, and usually they lack detectable blood flow. On color Doppler examination, the spectral curve analysis can unveil the type of flow within the channels. In the presence of very low-flow vascular malformations (<2 cm/s), vascularity may go undetected by the current machines. In contrast, high-flow vascular malformations show prominent and easily detectable blood flow. Ultrasound can guide percutaneous procedures such as embolization and monitor systemic or local treatments. Thus, MRI can be reserved for the cases that present multiple lesions and deep involvement[2,6,34–36] (Fig. 14).

Malignant Lesions

NonMelanoma Skin Cancer (NMSC)

This is the most common type of cancer in human beings and is composed of 2 main types: basal cell carcinoma (BCC) and

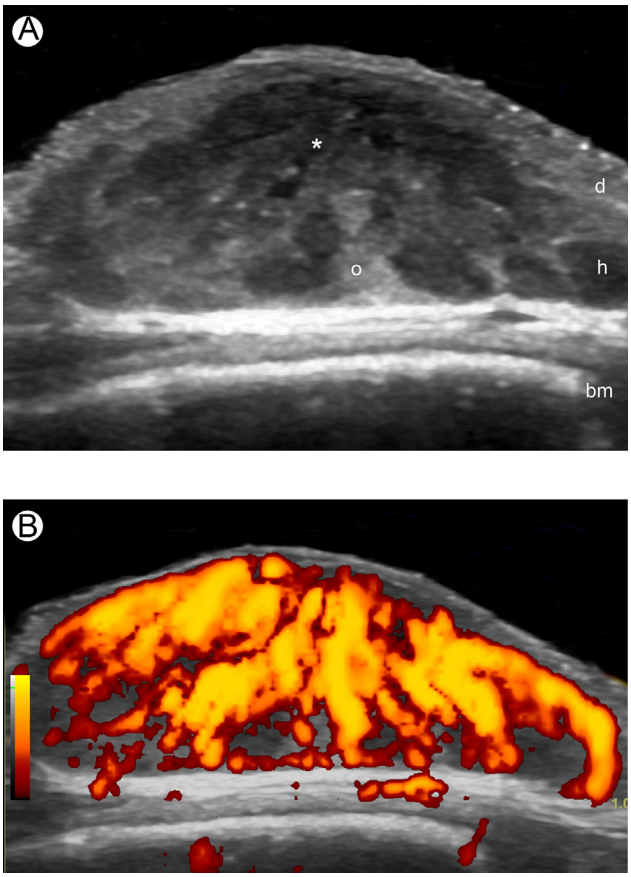

Figure 13 Hemangioma (proliferative phase). (A) Gray scale ultrasound (transverse view, occipital scalp) demonstrates ill-defined heterogeneous structure in the dermis and hypodermis. Notice the mixed echogenicity pattern with prominent hypoechoic areas (*) that correspond to the most proliferative zones and the hyperechoic areas (o) that represent an initial involution part. (B) Power Doppler and (C) 3D power angio reconstruction shows the highly vascular nature of the lesion. (Color version of figure is available online.)

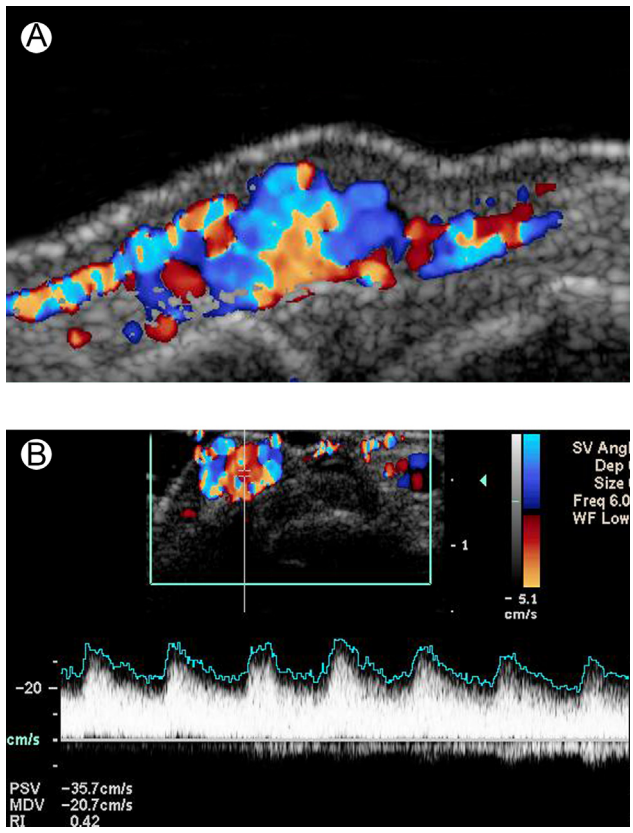

Figure 14 High-flow arterial vascular malformation. (A) Color Doppler ultrasound (longitudinal view, dorsum of the left index finger, metatarsophalangeal joint level) demonstrates hypervascular lesion with turbulent flow. (B) Spectral curve analysis shows arterial flow within the lesion (peak systolic velocity: 35.7 cm/s). (Color version of figure is available online.)

squamous cell carcinoma (SCC). BCC is the most frequent form and represents 75%-80% of NMSC. NMSC is more common in areas of the body highly exposed to the sun, such as the face which may complicate the cosmetic prognosis. Patients that present immunosuppressive diseases or treatments, including the recipients of renal transplants, show a higher incidence and more aggressive presentations of NMSC. Incomplete excisions of primary NMSC lesions have been reported in up to 67% of the cases of SCC, and up to 32% in BCC.[37–39] Histologically, BCC shows islands of atypical basaloid cells and fibrous stroma. Some subtypes show abundant mucin and a pseudoglandular appearance.[40] On sonography, BCC tends to show as well-defined, oval-shaped, hypoechoic lesions that commonly present hyperechoic spots. Increased vascularity (low flow) is usually detected within or surrounding the tumor. Occasionally, there are pleomorphic appearances of BCC that include asymmetric, lobulated or irregular presentations. There are 2 sonographic artifacts that have been reported in BCC lesions. One is called the "angles at the bottom" and is produced by significant inflammation due to dilated vessels and giant cells which can produce a hypoechoic angled band at the bottom of the lesion. The other artifact is called the "blurry tumor" and is caused by extensive hyperplasia of sebaceous glands which generate blurriness or almost isoechogenicity of the lesion with the surrounding tissue. The latter artifact has been detected on the tip of the nose. Nevertheless, both artifacts may be recognized by a well-trained operator.[2,6,41,42] SCC is a malignant tumor of keratinocytes and shows atypical squamous epithelium with variable degrees of mitosis and pleomorphism. On sonography, SCC shows as well-defined or irregular hypoechoic lesions without hyperechoic spots. Also, tumor hypervascularity with low-flow vessels may be detected. Besides the cutaneous layer involvement, cartilage or muscle layers may be affected in deeper NMSC tumors, especially in locations where the skin is thin such as in the nose, eyelids, lips, and ear pinna which can be detected by ultrasound[2,6] (Figs. 15 and 16).

Malignant Melanoma (MM)

This is the less frequent form of skin cancer (4%-11%) but presents the highest rate of mortality, causing 75% of cutaneous cancer–related deaths and provoking more

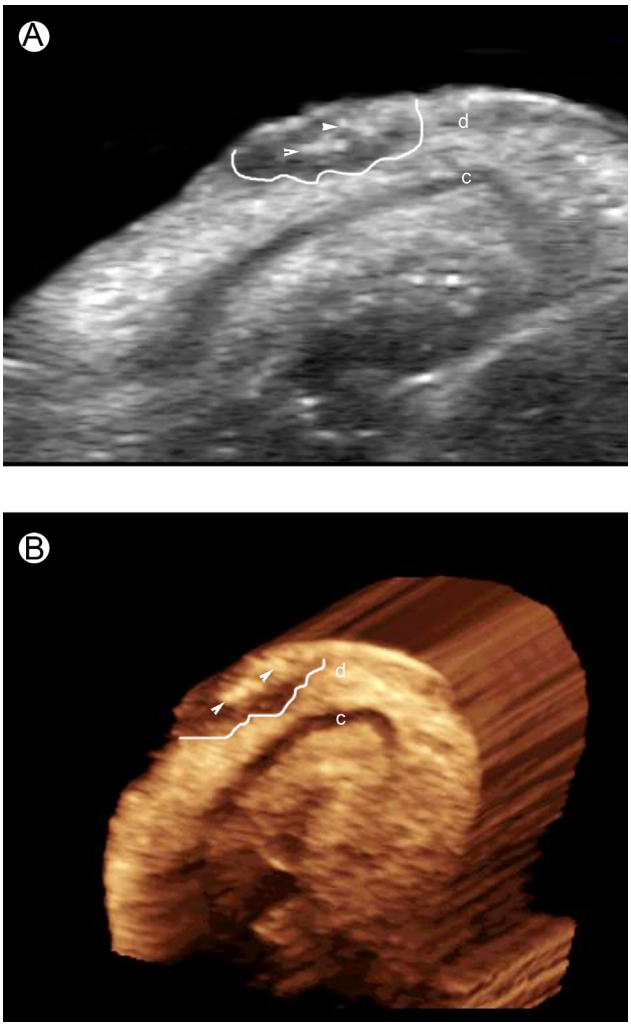

Figure 15 Basal cell carcinoma (posterior aspect of the left ear pinna). (A) Gray scale ultrasound and (B) 3D reconstruction (transverse view) demonstrate oval-shaped hypoechoic lesion (outlined) located in the dermis. There are hyperechoic spots (arrowheads) within the tumor. The auricular cartilage is unremarkable. d, dermis; c, auricular cartilage. (Color version of figure is available online.)

than 8000 deaths per year in the United States.[43] Melanoma recurrence has been reported in up to 35.9%, and can increase up to 46.1% when the head and neck region is considered.[44,45] Clinically, MMs commonly show as dark pigmented lesions. Histologically, MMs are composed of atypical melanocytes that present irregular nuclei, nuclear pleomorphism, and marked mitotic activity. Spindle or epitheliod cells can also be detected.[46] The prognosis of MM is based on the Breslow classification that reports the depth of involvement of this entity on histology, measuring from the granulous layer of the epidermis to the deepest part of the tumor. On sonography, MMs tend to show as well-defined, fusiform hypoechoic lesions with prominent vascularity. Sonography can discriminate between melanomas that measure $>$ or $<$ 1 mm (depth), which is important for deciding, for example on the performance of a sentinel node procedure that is indicated in melanomas that measure $>$ 1 mm. Also, sonography allows us to detect satellite ($<$ 2 cm from the primary tumor), in-transit ($\geq$ 2 cm from the primary tumor), or nodal metastases. Locoregional sonographic staging of melanomas has proven to be useful for detecting secondary involvement. Balloon shape, nodular thickening of the cortex and loss of hyperechogenicity of the medullae are signs of malignant nodal infiltration. The anechoic areas, frequently detected within the secondary lesions (extranodal or nodal), seem to be caused by the hypercellularity of the tumor rather than necrosis. The vascular density in melanoma has been correlated with the metastatic potential, and neovascularization has been reported as a prognostic factor for metastasis equivalent to the Breslow index[47–58] (Fig. 17).

Inflammatory Lesions

Psoriasis

This is an autoimmune disease that affects the skin, nails, tendons, entheses (ie, insertion sites of the tendons), and joints. Clinically, erythematous, scaly plaques in the skin as well as nail involvement such as pitting, discoloration, onycholysis (ie, separation of nail-plate from the nail bed), and subungual hyperkeratosis are commonly seen. On sonography, increased thickness, undulation of the epidermis

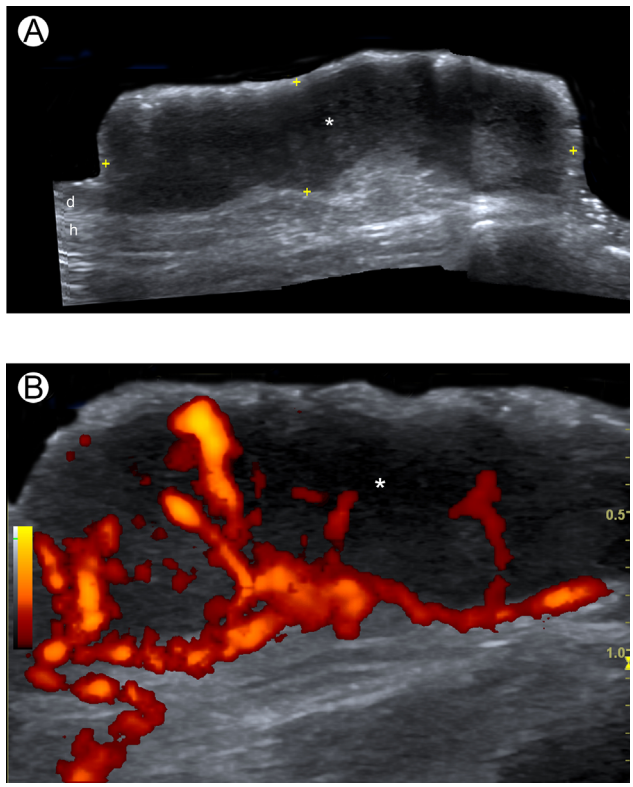

Figure 16 Squamous cell carcinoma (left cheek). (A) Gray scale ultrasound (extended field of longitudinal view) shows bulging hypoechoic lesion (*, between markers) that emerges from the dermis. (B) Power Doppler demonstrates increased blood flow with tortuous vessels within the lesion. d, dermis; h, hypodermis. (Color version of figure is available online.)

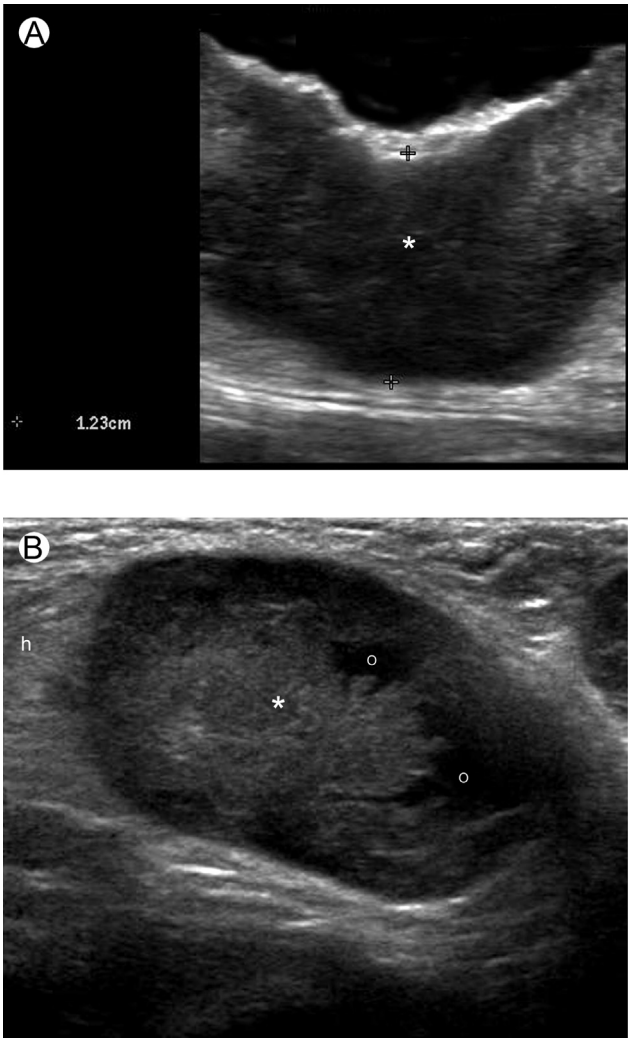

Figure 17 Melanoma. (A) Gray scale ultrasound (transverse view, at the abdominal wall) shows a 1.23 cm depth mainly hypoechoic lesion (*) located in the dermis and hypodermis. (B) Gray scale ultrasound (transverse view, right axilla) shows a well-defined, oval-shaped hypoechoic structure (*) located in the hypodermis that correspond to a nodal metastasis. Notice the anechoic areas (o) within the lesion. h, hypodermis.

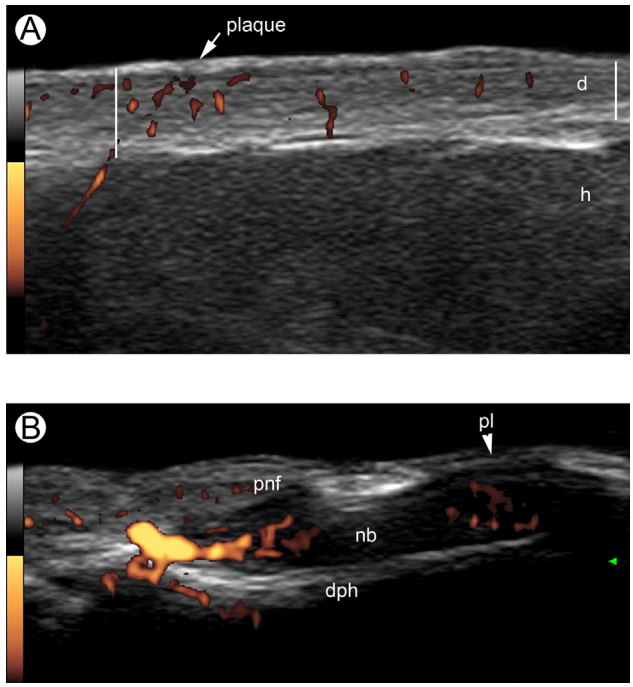

Figure 18 Psoriasis. (A) Power Doppler ultrasound (transverse view, abdominal wall) demonstrates increased thickness of the epidermis and dermis in the site of the plaque (large vertical white line). Increased dermal blood flow in the plaque region is also detected. A normal skin region (short vertical line) is seen in the right site of the figure. (B) Power Doppler ultrasound (longitudinal view, right index finger) shows increased vascularity within the nail bed. Increased thickness and irregularities in the nail plates as well as increased thickness of the nail bed are also detected. d, dermis; h, hypodermis; nb, nail bed; pnf, proximal nail fold; pl, nail plates; dph, distal phalanx. (Color version of figure is available online.)

and hypoechogenicity of the underlying upper dermis in the psoriatic plaques can be observed. In active phases, hypervascularity may be detected in the dermal area of the plaques. On the nails, the sonographic appearance may vary according to the phase of activity of the disease, usually showing from early to late phases: hypoechogenicity and increased thickness of the nail bed (ie, distance from the ventral plate to the bony margin of the distal phalanx), loss of definition of the ventral plate, hyperechoic deposits in the ventral plate, loss of definition of both plates, wavy and thickened plates. On color Doppler examination, ungual vascularity is commonly increased during the active phases, mainly in the proximal nail bed with low-flow arterial vessels. Patients with psoriatic onychopathy more commonly present joint involvement. Prominent and hypoechoic synovium, anechoic fluid, and periarticular erosions may be detected in the joints. Also, increased blood flow may be detected in the synovium during active phases. Tendinopathy signs that reveal hypoechoic or heterogeneous echogenicity of the tendons, which include the insertion sites (enthesis) have been reported in psoriatic patients even at subclinical stages. Sonography may support the diagnosis, assess the severity, and monitor the treatment in psoriasis[59–66] (Fig. 18).

Morphea

This is the cutaneous form of scleroderma, and a connective tissue disease. It comprises several subtypes and the most common is the dermal plaque-type, also called circumscribed plaque type of morphea. There are other subtypes and variants such as the deep form of morphea that can affect the hypodermis, fascia (eosinophilic fasciitis), and muscular layers. Other morphea variants are the guttate (drop-like) form, the atrophoderma of Pasini and Pierini type, the keloidal type, and the lichen sclerosis et atrophicus. The linear morphea is the most common form of presentation in children and can show as "en coup de sabre", progressive hemifacial atrophy (Parry-Romberg syndrome—PRS), or linear limb involvement.[67] On histology, the appearance can vary according to the phase and depth of involvement. During

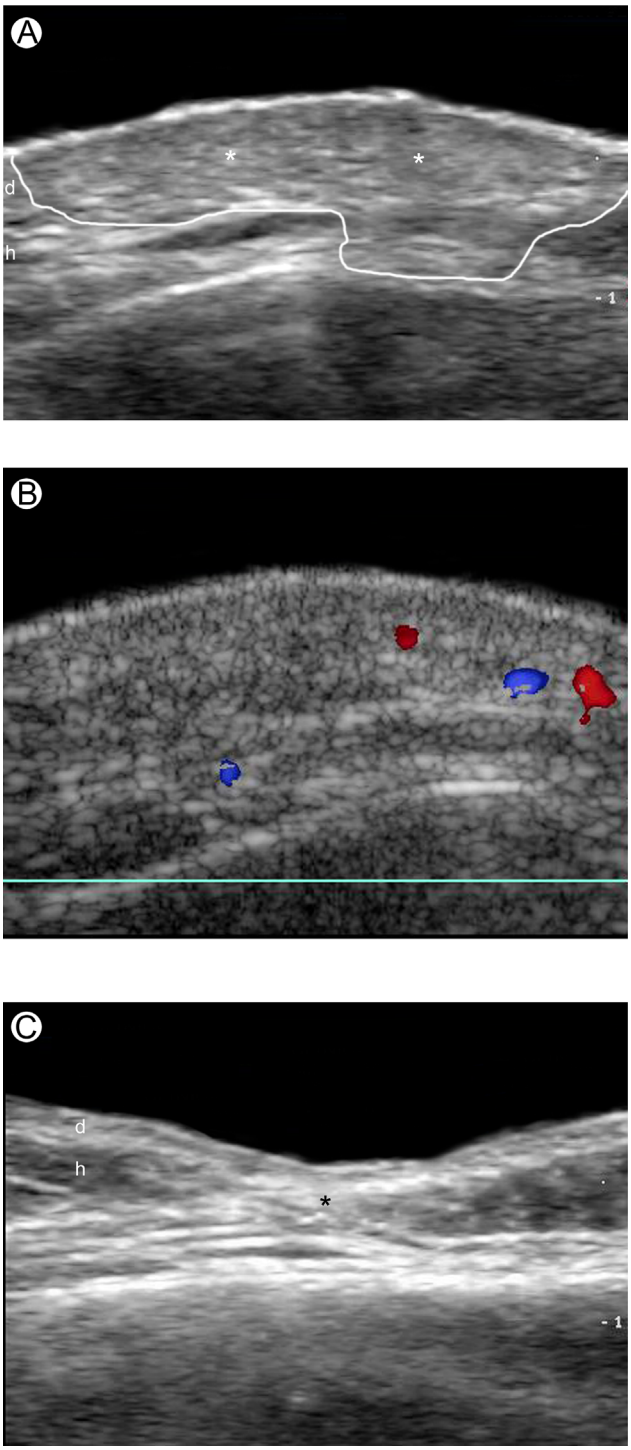

Figure 19 Morphea. (A, B) Morphea at inflammatory phase. (A) Gray scale ultrasound (transverse view, right cheek) shows increased thickness and slightly decreased echogenicity of the dermis (*, outlined). Increased echogenicity of part of the hypodermis is also detected. (B) Color Doppler ultrasound (transverse view) demonstrates a mild increase in the regional vascularity. (C) Morphea at phase of atrophy. Gray scale ultrasound (transverse view, right frontal region) shows decreased thickness of the dermis and hypodermis in the lesional region (*). Notice the lack of fatty lobules in the atrophy region. d, dermis; h, hypodermis. (Color version of figure is available online.)

the inflammation phase thick collagen bundles, perivascular inflammatory infiltrates (lymphocytes, plasma cells, and eosinophils) may be detected. At the end stage there is significant atrophy of eccrine glands, vessels and hypodermal fatty lobules, and thick dermal collagen bundles. On sonography, the appearance can also vary according to the phase of morphea. Thus, during the active inflammatory phase, increased thickness and decreased echogenicity of the dermis, as well as increased echogenicity of the hypodermis can be found. In the atrophic phase there is thinning of both dermis and hypodermis. On color Doppler, increased vascularity is detected in the dermis or hypodermis, or both during the active phase.[68–69] Cutaneous hypervascularity and increased echogenicity of the hypodermis have been reported as the most sensitive sonographic signs for assessing activity in morphea. Ipsilateral parotid gland inflammatory changes (hypoechogenicity or hypervascularity, or both) have been detected in concomitance with Parry-Romberg syndrome[70] (Fig. 19).

Hidradenitis Suppurativa

This is a chronic inflammatory disease characterized by recurrent abscesses, fistulae, and scarring that commonly involve the intertriginous skin that bears prominent hair follicles and apocrine glands. The most frequent locations affected by hidradenitis suppurativa are the axillae and groin.[71] On sonography, enlargement of the hair follicles, round- or oval-shaped anechoic pseudocystic dermal structures, hypoechoic dermal and hypodermal fluid collections, as well as fistulous tracts can be detected. Occasionally, hyperechoic lines that correspond to fragments of hair tracts are observed within the collections or fistulous tracts. Increased vascularity with low-flow vessels is usually found in the periphery of the collections or fistulae. Sonography allows mapping of the disease, provides anatomical data that

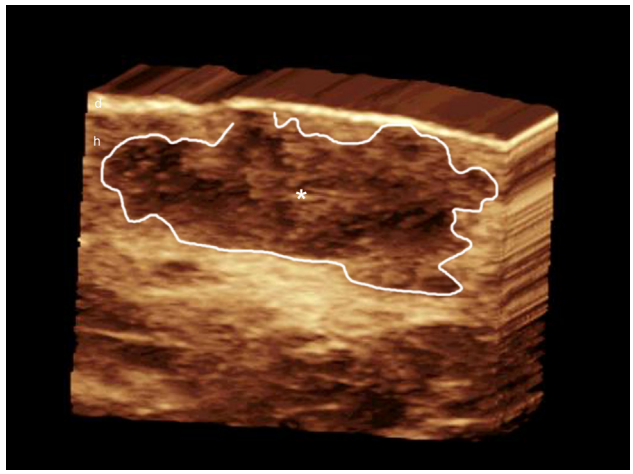

Figure 20 Hidradenitis suppurativa. 3D reconstruction (transverse view, right axilla) shows hypoechoic collection (*, outlined) located in the dermis and hypodermis. (Color version of figure is available online.)

can assess the severity and improve management of the disease[72,73] (Fig. 20).

Plantar Warts

These are generated by an infection with the human papilloma virus. Plantar warts can be very painful and therefore limit the daily activities of patients. Clinically, because of the exquisite pain, these lesions may be mistaken for a foreign body or Morton neuroma. On physical examination, they show as single or multiple hyperkeratotic lesions on the sole of the foot. Histologically, an endophytic proliferation of the virus is produced in the skin. On sonography, plantar warts show as well-defined, oval or fusiform shaped lesions located in the epidermis and dermis. Commonly, there is increased dermal blood flow at the bottom of the lesions with low-velocity arterial vessels and distention of the underlying plantar bursa. Sonography can support the diagnosis and management of these conditions[74,75] (Fig. 21).

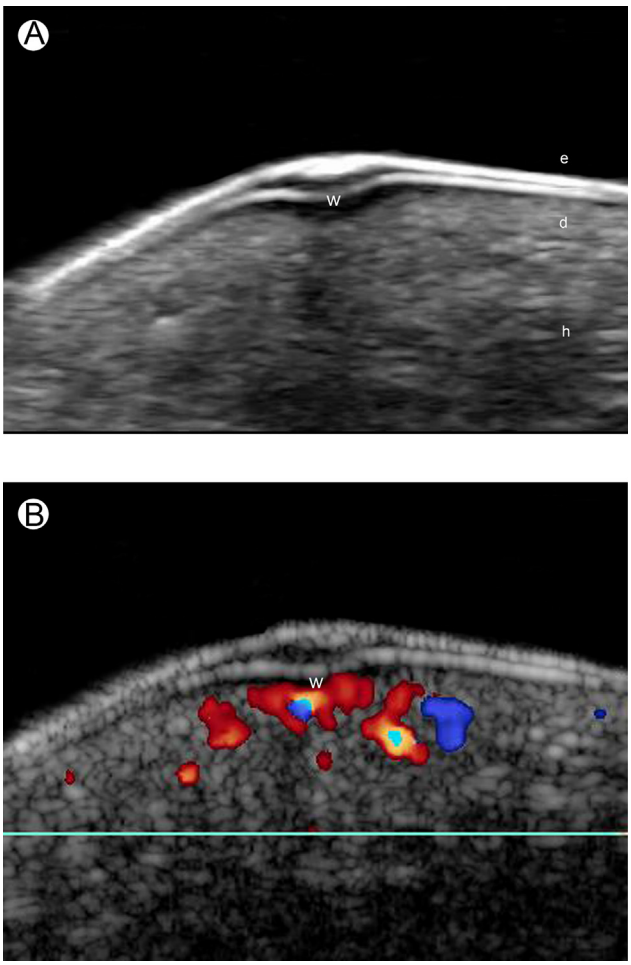

Figure 21 Plantar wart. (A) Gray scale ultrasound (longitudinal view, sole of the left foot) shows well-defined, oval-shaped fusiform hypoechoic lesion that involves epidermis and dermis. (B) Color Doppler ultrasound (longitudinal view) demonstrates increased vascularity in the dermal part of the wart. e, epidermis; d, dermis; h, hypodermis; w, wart. (Color version of figure is available online.)

Nail Pathology

Benign Lesions

Glomus Tumor

These benign tumors are generated in the neuromyoarterial plexus and the most common location is the nail bed. Clinically, they commonly present intense pain and sensitivity

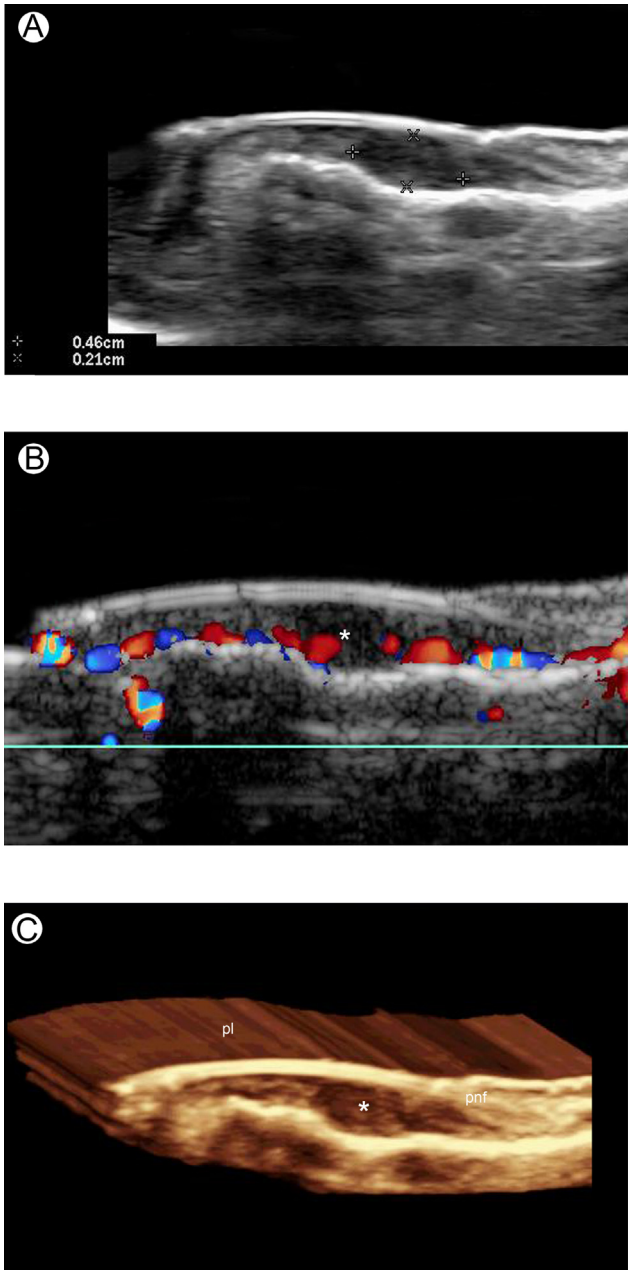

Figure 22 Glomus tumor. (A) Gray scale ultrasound (longitudinal view, left middle finger) shows a 4.6 mm (long) × 2.1 mm (depth) well-defined, oval-shaped hypoechoic nodule (*, between markers) in the proximal part of the nail bed. There is scalloping of the bony margin of the distal phalanx underlying the lesion and upward displacement of the nail plates on top of the tumor. (B) Color Doppler ultrasound (longitudinal view) demonstrates increased vascularity within the nodule (*). (C) 3D reconstruction (5-8 seconds sweep) highlights the glomus tumor. pl, nail plates; pnf, proximal nail fold. (Color version of figure is available online.)

to cold. Depending on the size and location, the tumor can affect the ungual matrix and produce secondary dystrophies in the nail plates.

On sonography, they show as well-defined, hypoechoic oval- or round-shaped structures in the nail bed. They are usually single and frequently affect the proximal part of the nail bed. Nevertheless, distally located forms of presentations can also be found. Scalloping of the underlying bony margin of the distal phalanx is a usual finding. On color Doppler, glomus tumors frequently present hypervascularity with slow-flow vessels[2,6,8,11,12,76–78] (Fig. 22).

Subungual Exostosis

These are outgrowths of bone that emerge from the bony margin of the distal phalanx and bulge into the nail bed or periungual region, or both. They present a wide range of clinical appearances that include subungual erythematous lumps, nail plate dystrophies or elevation, and periungual erythema, among others. Therefore, the patients are frequently referred for an ultrasound examination before an x-ray test. On sonography, subungual exostoses appear as hyperechoic band-like or linear structures connected to the bony margin of the distal phalanx. A hypoechoic cap can cover the hyperechoic bony outgrowth if there is cartilage on top of the bony structure (osteochondroma). Pronounced hypoechogenicity, thickening and increased blood flow within the nail bed may also be found as part of the reactive and usually long-term inflammatory process[2,6,8,12] (Fig. 23).

Granuloma

These are reactive lesions commonly secondary to trauma, and are composed of proliferative scarring and inflammation which generate a pseudomass effect. Clinically, they show a variable degree of nail dystrophy and ungual swelling. Granulomas can also affect the periungual skin and clinically show as reddish lumps in the proximal nail fold (usually the telangiectasic form). On sonography, subungual granulomas appear as ill-defined, hypoechoic areas in the nail bed that frequently involve the matrix region. Increased thickness of the nail bed is also commonly detected. Usually, the bony margin of the distal phalanx is unremarkable. In the periungual region they can present as hypoechoic round or oval shaped structures in the dermis of the proximal nail fold. The degree of vascularity of granulomas is variable and can go

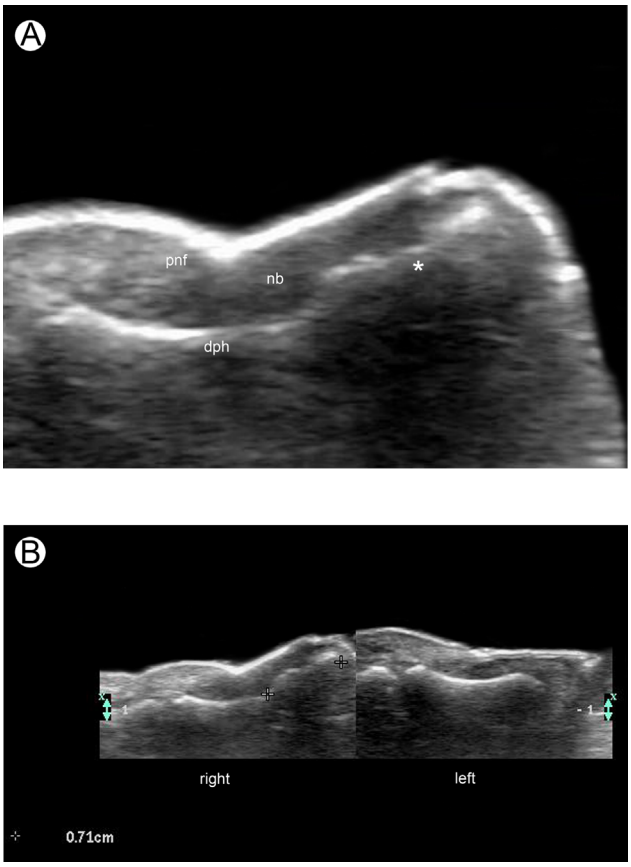

Figure 23 Subungual exostosis. (A, B) Gray scale ultrasounds (longitudinal views) of the right 3rd toenail. (A) An hyperechoic band (*) that emerges from the bony margin of the distal phalanx and bulges into the nail bed is detected. (B) Comparative side-by-side views demonstrates the subungual exostosis (7.1 mm long, between markers) only in the right side. nb, nail bed; dph, distal phalanx; pnf proximal nail fold.

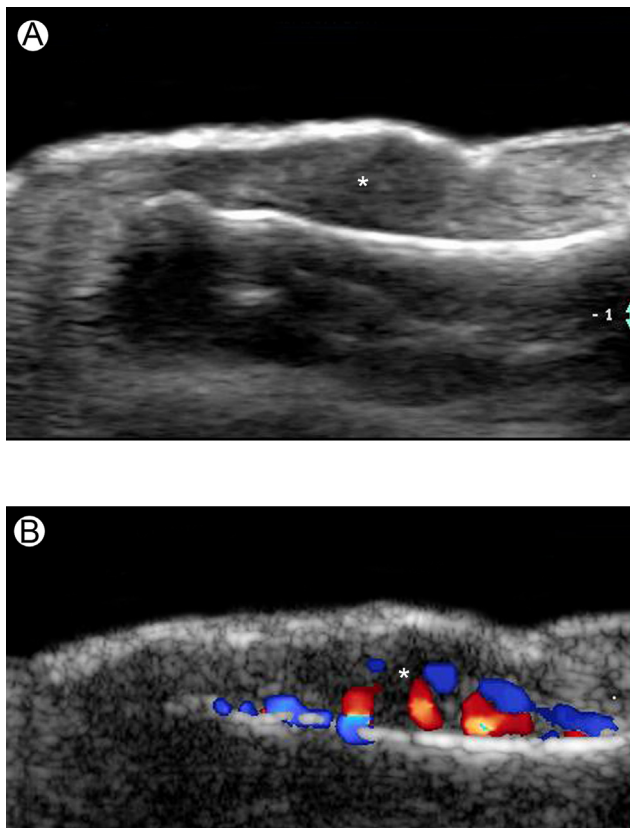

Figure 24 Subungual granuloma. (A) Gray scale ultrasound (longitudinal view, left thumb) shows ill-defined increased thickness and hypoechogenicity mainly affecting the 2 proximal thirds (*) of the nail bed which includes the matrix region. Upward displacement and thickening of the nail plates is also detected. The bony margin of the distal phalanx is unremarkable. (B) Color Doppler ultrasound (longitudinal view) demonstrates increased vascularity within the affected area (*). (Color version of figure is available online.)

from hypovascular to hypervascular (most common in the telangiectasic variant)[2,6,8,12] (Fig. 24).

Synovial Cysts

These are periungual cystic structures that are commonly generated by the leakage of synovial fluid from the distal interphalangeal joint into the periungual and ungual region. Thus, synovial cysts are usually connected to the distal interphalangeal joint. The most common location is the proximal nail fold, but they also may bulge into the nail bed and compress the ungual matrix. This latter compression can generate secondary dystrophies of the nail plates such as thickening, disruption, or irregularities. On sonography, they show as round- or oval-shaped anechoic cystic structures that commonly present a connecting thin and tortuous anechoic tract to the distal interphalangeal joint. Synovial anechoic fluid and osteophytes in the neighboring joint can also be detected. On color Doppler these cysts lack vascularity[2,6.8,12, 79] (Fig. 25).

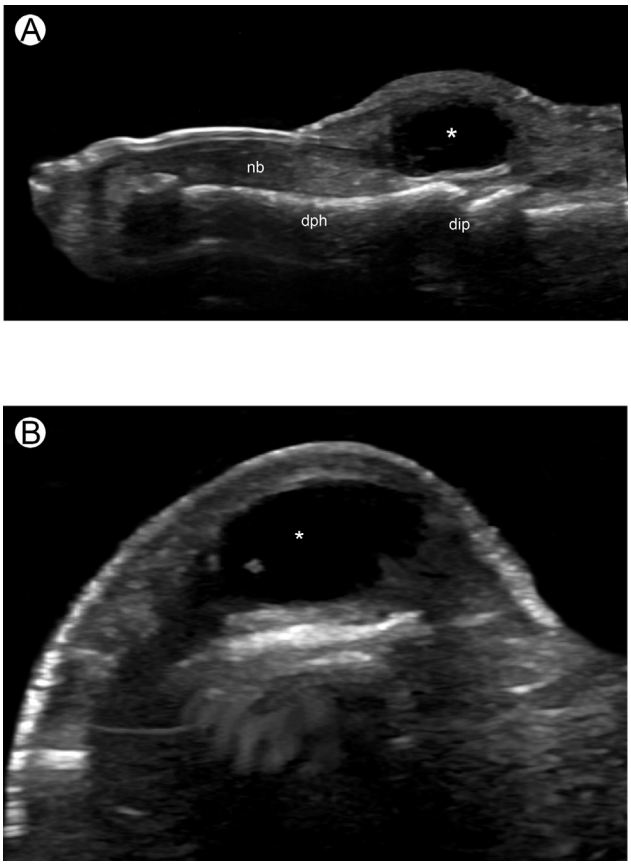

Figure 25 Synovial cyst. (A) Gray scale ultrasound (longitudinal view) demonstrates a well-defined, oval-shaped anechoic cystic structure (*) in the proximal nail fold and located on top of the distal interphalangeal joint. (B) Gray scale ultrasound shows the cystic structure (*) in transverse view. nb, nail bed; dph, distal phalanx; dip, distal interphalangeal joint.

Exogenous Materials

Foreign Bodies

These can be divided according to their nature, into organic (biological) and synthetic. Organic foreign bodies are derived from living organisms and examples can be splinters of wood, spines, or thorns of roses. Synthetic materials can be fragments of glass or metal. On sonography, foreign bodies appear as dermal or hypodermal, or both, hyperechoic laminar or bilaminar structures usually surrounded by hypoechoic granulomatous tissue. Synthetic foreign bodies usually produce a posterior acoustic reverberation artifact. Increased vascularity in the periphery of the foreign body is commonly detected as a result of the inflammatory reaction. Sonography can support the diagnosis, assess the nature and location, and lastly, guide the removal of the foreign body[2,6,80] (Fig. 26).

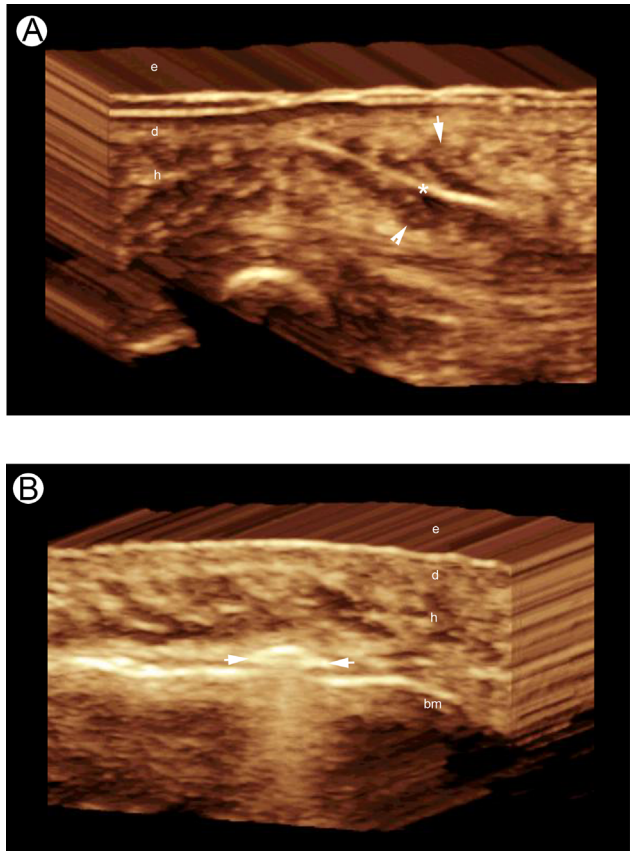

Figure 26 Foreign body. 3D reconstructions (5-8 seconds sweep). (A) Sea urchin spine (*) appears as a hyperechoic line (*) in the dermis and hypodermis of the sole of the right great toe. There is hypoechoic granulomatous tissue in the periphery of the spine. (B) Fragment of glass shows as a hyperechoic band (arrows) with posterior acoustic reverberation artifact located in the deep hypodermis of the right frontal region. e, epidermis; d, dermis; h, hypodermis; bm, bony margin of the frontal bone. (Color version of figure is available online.)

Figure 27 Hyaluronic acid. Gray scale ultrasound (transverse view, left periocular region) shows 2 oval-shaped, anechoic pseudocystic structures (arrows) in the hypodermis.

Fillers

These are particles that are used for cosmetic augmentation purposes such as the filling of wrinkles or plumping of the lips, or both. They can be classified according to their nature, or reabsorption capabilities into biological (degradable) or synthetic (nondegradable). Commonly, fillers are located in the hypodermis rather than the dermis, therefore the term "dermal fillers" is a confusing name. The most common biological filler is hyaluronic acid. This filler appears on sonography as round- or oval-shaped anechoic pseudocystic structures, usually in the hypodermis. Hyaluronic acid deposits decrease in size over time (3-6 months) until complete reabsorption. Examples of synthetic fillers are polymethyl methacrylate, calcium hydroxyapatite, polyacrylamide gel, and silicone (pure or oily forms). Polymethyl methacrylate appears on ultrasound as bright hyperechoic dots with mini-comet tail artifact (small posterior reverberation). Calcium hydroxyapatite shows on ultrasound as hyperechoic deposits with a posterior acoustic shadowing artifact which is due to the acoustic properties of calcium. Polyacrylamide gel shows on ultrasound as round- or oval-shaped anechoic pseudocystic structures that do not change in size for at least 18 months and are usually accompanied by increased echogenicity of the surrounding hypodermis. The silicone usage for cosmetic purposes is not approved by FDA but its usage has been reported in other countries. Pure silicone appears on sonography as oval-shaped anechoic deposits that do not modify in size over time. In contrast, silicone oil is hyperechoic and produces a strong posterior reverberation artifact, an appearance that has been called "snow storm". Sonography can assist the detection and identification of the type of filler, and this may be critical when dealing with adverse reactions to these compounds that sometimes can present confusing clinical signs and may mimic other common dermatologic conditions[2,81–85] (Figs. 27-31).

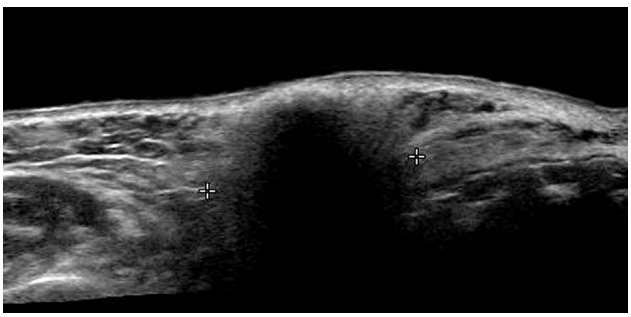

Figure 28 Calcium hydroxyapatite. Gray scale ultrasound (transverse view, right nasofold region) demonstrates hyperechoic band (*) in the dermis with a strong posterior acoustic shadowing artifact (between markers).

Figure 29 Polymethyl methacrylate (PMMA). Gray scale ultrasound shows several bright hyperechoic dots with mini-comet tail artifact (arrows) located in the dermis and hypodermis of the right gluteal region.

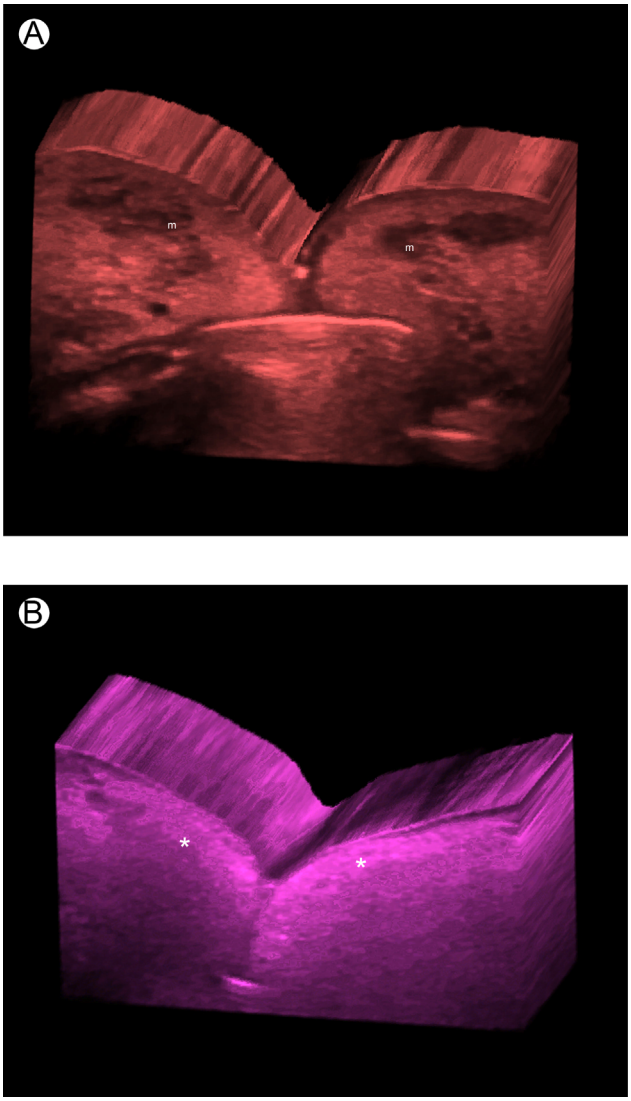

Figure 30 Silicone oil. 3D reconstructions (gray scale with color filtering, longitudinal views of the lips). (A) Normal lips (for comparison). (B) Lips with silicone oil. Notice the hyperechoic deposits (*) with "snow storm" appearance in the dermis of both lips that also involves the orbicularis muscles. m, orbicularis muscle of the lip. (Color version of figure is available online.)

Conclusion

Sonography can support the diagnosis and management in common cutaneous and ungual entities. It may help surgical or medical treatment planning, or both, therefore can potentially prevent recurrences. Ultrasound can discriminate between a dermatologic and nondermatologic origin, as well as between endogenous and exogenous components. It can support the assessment of the activity and severity of common cutaneous diseases. Lastly, early knowledge of this detailed anatomical information can improve the cosmetic prognosis.

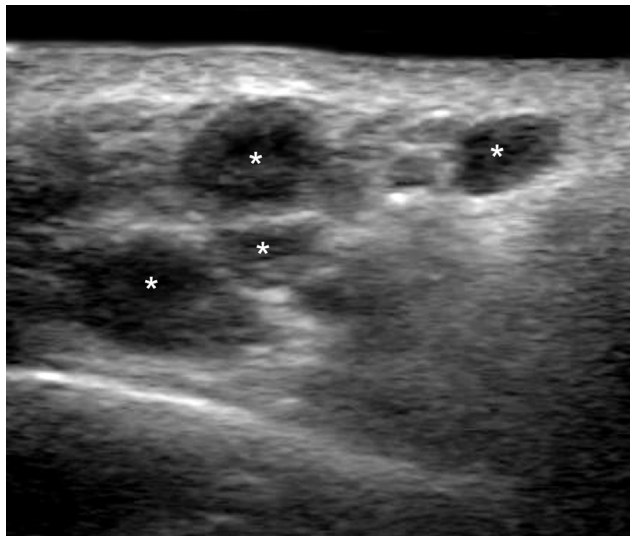

Figure 31 Polyacrylamide gel (PAAG). Gray scale ultrasound (longitudinal view, left nasofold region) demonstrates several oval-shaped, anechoic pseudocystic structures (*) in the hypodermis. A mild increase of the echogenicity of the surrounding hypodermal tissue is also detected.

References

1. Farinelli N, Berardesca E: The skin integument: Variation relative to sex, age, race, and body region. In: Serup J, Jemec GBE, Grove GL (eds): Handbook of Non-Invasive Methods and the Skin, (ed2) Boca Raton, FL, Taylor & Francis, 27-31, 2006
2. Wortsman X: Common applications of dermatologic sonography. J Ultrasound Med1 31 (1):97-111, 2012
3. Fornage BD, McGavran MH, Duvic M, et al: Imaging of the skin with 20-MHz US. Radiology 189:69-76, 1993
4. Desai TD, Desai AD, Horowitz DC, et al: The use of high-frequency ultrasound in the evaluation of superficial and nodular basal cell carcinomas. Dermatol Surg 33:1220-1227, 2007
5. Wortsman X, Wortsman J: Clinical usefulness of variable-frequency ultrasound in localized lesions of the skin. J Am Acad Dermatol 62:247-256, 2010
6. Wortsman X: Sonography of cutaneous and ungual lumps and bumps. Ultrasound Clin 2012. doi:http://dx.doi.org/10.1016/j.cult.2012.08.006
7. Aldrete JA: Modifications to the post anesthesia score for use in ambulatory surgery. J Perianesth Nurs 13:148-155, 1998
8. Wortsman X, Wortsman J, Soto R, et al: Benign tumors and pseudotumors of the nail: A novel application of sonography. J Ultrasound Med 29:803-816, 2010
9. Wortsman X, Wortsman J, Matsuoka L, et al: Sonography in pathologies of scalp and hair. Br J Radiol 85:647-655, 2012
10. Gniadecka M: Effects of ageing on dermal echogenicity. Skin Res Technol 7:204-207, 2001
11. Wortsman X, Jemec GBE: Ultrasound imaging of nails. Dermatol Clin 24:323-328, 2006
12. Thomas L, Vaudaine M, Wortsman X, et al: Imaging the nail unit. In: Baran R, de Berker D, Holzberg M, Thomas L (eds): Baran & Dawber's Diseases of the Nails and their Management, ed 4 Wiley-Blackwell, 132-153, 2012
13. Al-Nuaimi Y, Baier G, Watson RE, et al: The cycling hair follicle as an ideal systems biology research model. Exp Dermatol 19:707-713, 2010
14. Yagyu K, Hayashi K, Chang SC: Orientation of multi-hair follicles in nonbald men: Perpendicular versus parallel. Dermatol Surg 32:651-660, 2006

15. Seery GE: Surgical anatomy of the scalp. Dermatol Surg 28:581-587, 2002
16. Jin W, Ryu KN, Kim GY, et al: Sonographic findings of ruptured epidermal inclusion cysts in superficial soft tissue: Emphasis on shapes, pericystic changes, and pericystic vascularity. J Ultrasound Med 27:171-176, 2008
17. Huang CC, Ko SF, Huang HY, et al: Epidermal cysts in the superficial soft tissue: Sonographic features with an emphasis on the pseudotestis pattern. J Ultrasound Med 30:11-17, 2011
18. Yuan WH, Hsu HC, Lai YC, et al: Differences in sonographic features of ruptured and unruptured epidermal cysts. J Ultrasound Med 31:265-272, 2012
19. Folpe AL, Reisenauer AK, Mentzel T, et al: Proliferating trichilemmal tumors: Clinicopathologic evaluation is a guide to biologic behavior. J Cutan Pathol 30:492-498, 2003
20. Chang SJ, Sims J, Murtagh FR, et al: Am J Neuroradiol 27:712-714, 2006
21. Harlak A, Mentes O, Kilic S, et al: Sacrococcygeal pilonidal disease: Analysis of previously proposed risk factors. Clinics 65:125-131, 2010
22. Mentes O, Oysul A, Harlak A, et al: Ultrasonography accurately evaluates the dimension and shape of the pilonidal sinus. Clinics 64:189-192, 2009
23. Roche NA, Monstrey SJ, Matton GE: Pilomatricoma in children: Common but often misdiagnosed. Acta Chir Belg 110:250-254, 2010
24. Hwang JY, Lee SW, Lee SM: The common ultrasonographic features of pilomatricoma. J Ultrasound Med 24:1397-1402, 2005
25. Choo HJ, Lee SJ, Lee YH, et al: Pilomatricomas: The diagnostic value of ultrasound. Skeletal Radiol 39:243-250, 2010
26. Solivetti FM, Elia F, Drusco A, et al: Epithelioma of Malherbe: New ultrasound patterns. J Exp Clin Cancer Res 29:42, 2010
27. Wortsman X, Wortsman J, Arellano J, et al: Pilomatrixomas presenting as vascular tumors on color Doppler ultrasound. J Pediatr Surg 45:2094-2098, 2010
28. Hassanein AH, Alomari AI, Schmidt BA, et al: Pilomatrixoma imitating infantile hemangioma. J Craniofac Surg 22:734-736, 2011
29. MacKee P, Calonje E, Granter S: Tumors of fibrous and myofibroblastic tissue. In: MacKee P, Calonje E, Granter S (eds): Pathology of the Skin With Clinical Correlation, ed 3 St. Louis, MO, Elsevier Mosby, 1669-1723, 2005
30. Mulliken JB, Glowacki J: Hemangiomas and vascular malformations in infants and children: A classification based on endothelial characteristics. Plast Reconstr Surg 69:412-422, 1982
31. Enjolras O: Classification and management of the various superficial vascular anomalies: Hemangiomas and vascular malformations. J Dermatol 24:701-710, 1997
32. Dubois J, Patriquin HB, Garel L, et al: Soft tissue hemangiomas in infants and children: Diagnosis using Doppler sonography. Am J Roentgenol 171:247-252, 1998
33. Paltiel HJ, Burrows PE, Kozakewich HPW, et al: Soft tissue vascular anomalies: Utility of US for diagnosis. Radiology 214:747-754, 2000
34. Puig S, Casati B, Staudenherz A, et al: Vascular low-flow malformations in children: Current concepts for classification, diagnosis and therapy. Eur J Radiol 53:35-45, 2005
35. Trop I, Dubois J, Guibaud L, et al: Soft tissue venous malformations in pediatric and young adult patients: Diagnosis with Doppler US. Radiology 212:841-845, 1999
36. Dubois J, Soulez G, Oliva VL, et al: Soft-tissue venous malformations in adult patients: Imaging and therapeutic issues. Radiographics 21:1519-1531, 2001
37. Gniadecki R, Normal Dam T: Basal cell carcinoma—Clinical guidelines, Danish Dermatological Society. Forum Nord Derm Ven 14:4-6, 2009
38. Matteucci P, Pinder R, Magdum A, et al: Accuracy in skin lesion diagnosis and the exclusion of malignancy. J Plast Reconstr Aesthet Surg 64:1460-1465, 2011
39. Santiago F, Serra D, Vieira R, et al: Incidence and factors associated with recurrence after incomplete excision of basal cell carcinomas: A study of 90 cases. J Eur Acad Dermatol Venereol 24:1421-1424, 2010
40. Brenn T, Mc Kee P: Tumors of the surface epithelium. In: Mc Kee P, Calonje E, Granter S (eds): Pathology of the Skin with Clinical Correlations, ed 3 St. Louis, MO, Elsevier Mosby, 1167-1182, 2005
41. Bobadilla F, Wortsman X, Muñoz C: Pre-surgical high resolution ultrasound of facial basal cell carcinoma: Correlation with histology. Cancer Imaging 8:163-172, 2008
42. Uhara H, Hayashi K, Koga H, et al: Multiple hypersonographic spots in basal cell carcinoma. Dermatol Surg 33:1215-1219, 2007
43. Ekwueme DU, Guy G, Li C, et al: The health burden and economic costs of cutaneous melanoma mortality by race/ethnicity—United States, 2000 to 2006. J Am Acad Dermatol 6 (Suppl.1):S133-S143, 2011
44. Reintgen DS, Vollmer R, Tso CY, et al: Prognosis for recurrent stage I malignant melanoma. Arch Surg 122:1338-1342, 1987
45. Nazarian LN, Alexander AA, Kurtz AB, et al: Superficial melanoma metastases: Appearances on gray-scale and color Doppler sonography. AJR Am J Roentgenol 170:459-463, 1998
46. McKee P, Calonje E, Granter S: Melanoma. In: MacKee P, Calonje E, Granter S (eds): Pathology of the Skin with Clinical Correlations, ed 3 St. Louis, MO, Elsevier Mosby, 1309-1356, 2005
47. Wortsman X: Sonography of the primary cutaneous melanoma: A review. Radiol Res Pract 2012:814396, 2012
48. Tacke J, Haagen G, Horstein O, et al: Clinical relevance of sonometry-derived tumour thickness in malignant melanoma—A statistical analysis. Br J Dermatol 132:209-214, 1995
49. Catalano O, Siani A: Cutaneous melanoma: Role of ultrasound in the assessment of locoregional spread. Curr Probl Diagn Radiol 39:30-36, 2010
50. Vilana R, Puig S, Sanchez M, et al: Preoperative assessment of cutaneous melanoma thickness using 10-MHz sonography. AJR Am J Roentgenol 193:639-643, 2009
51. Music MM, Hertl K, Kadivec M, et al: Pre-operative ultrasound with a 12-15 MHz linear probe reliably differentiates between melanoma thicker and thinner than 1 mm. J Eur Acad Dermatol Venereol 24:1105-1108, 2010
52. Lassau N, Mercier S, Koscielny S, et al: Prognostic value of high-frequency sonography and color Doppler sonography for the preoperative assessment of melanomas. AJR Am J Roentgenol 172:457-461, 1999
53. Lassau N, Koscielny S, Avril MF, et al: Prognostic value of angiogenesis evaluated with high-frequency and color Doppler sonography for preoperative assessment of melanomas. AJR Am J Roentgenol 178:1547-1551, 2002
54. Voit C, Van Akkooi AC, Schäfer-Hesterberg G, et al: Ultrasound morphology criteria predict metastatic disease of the sentinel nodes in patients with melanoma. J Clin Oncol 28:847-852, 2010
55. Nazarian L, Alexander AA, Rawool NM, et al: Malignant melanoma: Impact of superficial US on management. Radiology 199:273-277, 1996
56. Catalano O, Voit C, Sandomenico F, et al: Previously reported sonographic appearances of regional melanoma metastases are not likely due to necrosis. J Ultrasound Med 30:1041-1049, 2011
57. Clemente-Ruiz de Almiron A, Serrano-Ortega S: Risk factors for in-transit metastasis in patients with cutaneous melanoma. Acta Dermosifiliogr 103:207-213, 2012; [Spanish]
58. Lassau N, Chami L, Chebil M, et al: Dynamic contrast-enhanced ultrasonography (DCE-US) and anti-angiogenic treatments. Discov Med 11:18-24, 2011
59. Johnson MA, Armstrong AW: Clinical and histologic diagnostic guidelines for psoriasis: A critical review. Clin Rev Allergy Immunol 2012 Jan 27; [Epub ahead of print]. doi: 10.1007/s12016-012-8305-3. PMID: 22278173.
60. Baran R: The burden of nail psoriasis: An introduction. Dermatology 221 (suppl 1):1-5, 2010
61. Wortsman X, Holm EA, Jemec GBE, et al: 15 MHz high resolution ultrasound examination of psoriatic nails. Rev Chil Radiol 10:6-9, 2004; [Spanish]
62. Gutierrez M, Wortsman X, Filippucci E, et al: High-frequency sonography in the evaluation of psoriasis: Nail and skin involvement. J Ultrasound Med 28:1569-1574, 2009
63. Gisondi P, Idolazzi L, Girolomoni G: Ultrasonography reveals nail thickening in patients with chronic plaque psoriasis. Arch Dermatol Res 304:727-732, 2012
64. Gutierrez M, De Angelis R, Bernardini ML, et al: Clinical, power Doppler sonography and histological assessment of the psoriatic

plaque: Short-term monitoring in patients treated with etanercept. Br J Dermatol 164:33-37, 2011
65. Kaeley GS: Review of the use of ultrasound for the diagnosis and monitoring of enthesitis in psoriatic arthritis. Curr Rheumatol Rep 13:338-345. doi:http://dx.doi.org/10.1007/s11926-011-0184-8
66. De Agustin JJ, Moragues C, de Miguel E, et al: A multicentre study on high-frequency ultrasound evaluation of the skin and joints in patients with psoriatic arthritis treated with infliximab. Clin Exp Rheumatol Sep:27, 2012
67. Fett N, Werth VP: Update on morphea: Part I. Epidemiology, clinical presentation, and pathogenesis. J Am Acad Dermatol. 64:217-228, 2011
68. Li SC, Liebling MS, Haines KA: Ultrasonography is a sensitive tool for monitoring localized scleroderma. Rheumatology (Oxford) 46:1316-1319, 2007
69. Li SC, Liebling MS: The use of Doppler ultrasound to evaluate lesions of localized scleroderma. Curr Rheumatol Rep 11:205-211, 2009
70. Wortsman X, Wortsman J, Sazunic I, et al: Activity assessment in morphea using color Doppler ultrasound. J Am Acad Dermatol 65:942-948, 2011
71. Jemec GB: Clinical practice. Hidradenitis suppurativa. N Engl J Med 366:158-164, 2012
72. Wortsman X, Jemec GB: Real-time compound imaging ultrasound of hidradenitis suppurativa. Dermatol Surg 33:1340-1342, 2007
73. Kelekis NL, Efstathopoulos E, Balanika A, et al: Ultrasound aids in diagnosis and severity assessment of hidradenitis suppurativa. Br J Dermatol 162:1400-1402, 2010
74. Wortsman X, Sazunic I, Jemec GB: Sonography of plantar warts: Role in diagnosis and treatment. J Ultrasound Med 28:787-793, 2009
75. Wortsman X, Jemec GB, Sazunic I: Anatomical detection of inflammatory changes associated with plantar warts by ultrasound. Dermatology 220:213-217, 2010
76. Wortsman X, Jemec GB: Role of high-variable frequency ultrasound in preoperative diagnosis of glomus tumors: A pilot study. Am J Clin Dermatol 10:23-27, 2009
77. Chen SH, Chen YL, Cheng MH, et al: The use of ultrasonography in preoperative localization of digital glomus tumors. Plast Reconstr Surg 112:115-119, 2003
78. Matsunaga A, Ochiai T, Abe I, et al: Subungual glomus tumour: Evaluation of ultrasound imaging in preoperative assessment. Eur J Dermatol 17:67-69, 2007
79. Wortsman X, Wortsman J: Skin ultrasound. In: Dogra V, Gaitini D (eds): Musculoskeletal Ultrasound with CT and MRI correlation, ed 1 Thieme, 2010147-170, 2010; [Chapter 9]
80. Creel SA, Girish G, Jamadar DA, et al: Sonographic surface localization of subcutaneous foreign bodies and masses. J Clin Ultrasound 37:158-160, 2009
81. Wortsman X, Wortsman J, Orlandi C, et al: Ultrasound detection and identification of cosmetic fillers in the skin. J Eur Acad Dermatol Venereol 26:292-301, 2012
82. Wortsman X, Wortsman J: Polyacrylamide fillers on skin ultrasound. J Eur Acad Dermatol Venereol 26:660-661, 2012
83. Wortsman X, Wortsman J: Sonographic outcomes of cosmetic procedures. AJR Am J Roentgenol 197:W910-W918, 2011
84. Hevia O: Six-year experience using centistokes silicone oil in 916 patients for soft tissue augmentation in a private practice setting. Dermatol Surg 35:1646-1652, 2009
85. Jacinto SS: Ten-year experience using injectable silicone oil for soft tissue augmentation in the Philippines. Dermatol Surg 31:1550-1554, 2005